Received: 29 June 2023 | Revised: 7 December 2023 | Accepted: 11 December 2023

DOI: 10.1111/mmi.15215

RESEARCH ARTICLE

WILEY

The *Plasmodium falciparum* CCCH zinc finger protein MD3 regulates male gametocytogenesis through its interaction with RNA-binding proteins

Afia Farrukh[1] | Jean Pierre Musabyimana[1] | Ute Distler[2] | Vanessa Jil Mahlich[1] | Julius Mueller[1] | Fabian Bick[1] | Stefan Tenzer[2] | Gabriele Pradel[1] | Che Julius Ngwa[1]

[1]Division of Cellular and Applied Infection Biology, Institute of Zoology, RWTH Aachen University, Aachen, Germany

[2]Core Facility for Mass Spectrometry, Institute of Immunology, University Medical Centre of the Johannes-Gutenberg University, Mainz, Germany

Correspondence
Gabriele Pradel, Division of Cellular and Applied Infection Biology, Institute of Zoology, RWTH Aachen University, Worringerweg 1, 52074 Aachen, Germany.
Email: pradel@bio2.rwth-aachen.de

Funding information
Deutsche Forschungsgemeinschaft, Grant/Award Number: NG170/1-1, PR905/15-1, PR905/19-1, PR905/20-1 and TE599/9-1; Deutscher Akademischer Austauschdienst

Abstract

The transmission of malaria parasites to mosquitoes is dependent on the formation of gametocytes. Once fully matured, gametocytes are able to transform into gametes in the mosquito's midgut, a process accompanied with their egress from the enveloping erythrocyte. Gametocyte maturation and gametogenesis require a well-coordinated gene expression program that involves a wide spectrum of regulatory proteins, ranging from histone modifiers to transcription factors to RNA-binding proteins. Here, we investigated the role of the CCCH zinc finger protein MD3 in *Plasmodium falciparum* gametocytogenesis. MD3 was originally identified as an epigenetically regulated protein of immature gametocytes and recently shown to be involved in male development in a barcode-based screen in *P. berghei*. We report that MD3 is mainly present in the cytoplasm of immature male *P. falciparum* gametocytes. Parasites deficient of MD3 are impaired in gametocyte maturation and male gametocytogenesis. BioID analysis in combination with co-immunoprecipitation assays unveiled an interaction network of MD3 with RNA-binding proteins like PABP1 and ALBA3, with translational initiators, regulators and repressors like eIF4G, PUF1, NOT1 and CITH, and with further regulators of gametocytogenesis, including ZNF4, MD1 and GD1. We conclude that MD3 is part of a regulator complex crucial for post-transcriptional fine-tuning of male gametocytogenesis.

KEYWORDS
CCCH zinc finger protein, exflagellation, malaria, male gametocytogenesis, *Plasmodium falciparum*, RNA-binding protein

1 | INTRODUCTION

Malaria is a life-threatening tropical disease caused by parasites of the genus *Plasmodium*, which accounts for over 249 million infections and 608,000 deaths in 2022. Among the five species of *Plasmodium* that infect humans, *Plasmodium falciparum* is the most lethal and responsible for the majority of malaria-related deaths particularly in WHO global Africa. To date, malaria eradication is being hampered

Gabriele Pradel and Che Julius Ngwa shared contribution.

by the rapid spread of resistance against frontline drugs, limited efficacy of the available malaria vaccine RTS, S and risk of disease aggravation due to climate change (Mora et al., 2022; WHO World Malaria Report, 2023). While the clinical symptoms and pathology of malaria are primarily associated with the asexual blood stages of the parasite, the sexual stages, particularly the gametocytes, play a critical role in transmission of the disease.

Plasmodium falciparum gametocytes are sexual precursors of the parasite that develop within the human host's bloodstream. These highly specialized cells are responsible for the production of male and female gametes following their uptake by the *Anopheles* mosquito vector, a process that requires their egress from the enveloping red blood cell (RBC). Formation and maturation of *P. falciparum* gametocytes in the human blood takes roughly 10 days. Gametocyte development is a tightly regulated process that involves complex molecular mechanisms of gene regulation, which drive sexual commitment and the morphological and physiological changes in the gametocytes including sex determination, and which also prime the gametocytes for gametogenesis (reviewed in, e.g., Bennink et al., 2016).

Transcriptional control plays a major role in both sexual commitment and sex determination. The gametocyte development protein 1 (GDV1) acts as a key regulator of sexual commitment by facilitating dissociation of heterochromatin protein 1 (HP1) from heterochromatic DNA at the genomic locus encoding AP2-G, the master transcription factor of gametocytogenesis (e.g., Brancucci et al., 2014; Coleman et al., 2014; Filarsky et al., 2018; Usui et al., 2019). AP2-G belongs to a group of ApiAP2 transcription factors that is involved in the regulation of gene expression during sexual development (e.g., Bancells et al., 2019; Josling et al., 2020; Kafsack et al., 2014; Poran et al., 2017; Sinha et al., 2014; van Biljon et al., 2019). Other ApiAP2 proteins of this group include AP2-G2 and AP2-G3, which co-regulate gametocytogenesis in conjunction with AP2-G (Modrzynska et al., 2017; Xu et al., 2021; Yuda et al., 2015; Zhang et al., 2017), and AP2-G5, which is essential for gametocyte maturation by downregulation of *ap2-g* expression (Shang et al., 2021). Two other ApiAP2 domain transcription factors, AP2-FG and AP2-O3, subsequently contribute to sex determination. While AP2-FG binds to the promoters of many female-specific genes and is thus required for the establishment of the full female gene expression profile, AP2-O3 acts as a repressor that targets male genes in female gametocytes as a means of safeguarding the female-specific transcriptome (Li et al., 2021; Yuda et al., 2020).

In addition to transcriptional regulation by ApiAP2 proteins, post-transcriptional mechanisms are responsible for gametocyte formation and sex differentiation. RNA-binding proteins play a critical role in the timely regulation of mRNA and protein synthesis during lifecycle progression of the parasite, including gametocytogenesis (reviewed in, e.g., Cui et al., 2015; Bennink & Pradel, 2019; Goyal et al., 2022). A series of RNA-binding proteins have been identified in *Plasmodium*, e.g., RNA helicases, zinc finger proteins (ZFPs; exhibiting C3H1 and C2H2 motifs), or members of the K homology (KH), Pumilio and Fem-3 binding factor (PUF) and acetylation lowers binding affinity (ALBA) families (Reddy et al., 2015). While the function of most of these RNA-binding proteins is yet unknown, some proteins have been assigned to translationally regulating the intraerythrocytic replication cycle, e.g., the DNA/RNA-binding protein ALBA1 and the two m^6A-mRNA-binding YTH domain proteins YTH.1 and YTH.2 (Baumgarten et al., 2019; Sinha et al., 2021; Vembar et al., 2015). Others have been linked to stage conversion and transmission, e.g., ALBA4 with crucial functions in gametocytes and sporozoites of the rodent malaria parasite *P. yoelii* (Munoz et al., 2017), or PUF1 and PUF2 of *P. falciparum*, which are involved in gametocyte maturation and sex differentiation (Miao et al., 2010; Shrestha et al., 2016).

Of particular importance for human-to-mosquito transmission are RNA-binding proteins that act as translational repressors, allowing the gametocytes to rapidly react to external stimuli following their transmission to mosquitoes. The repressed transcripts are bound in messenger ribonucleoprotein particles (mRNPs), which condense to cytosolic aggregations. They are particularly present in female gametocytes, where they store mRNAs that encode proteins required for the development of the mosquito midgut stages and which are introduced to protein synthesis at the onset of gametogenesis (reviewed in, e.g., Bennink et al., 2016; Bennink & Pradel, 2019). A prominent repressor protein originally identified in female *P. berghei* gametocytes is DOZI (development of zygote inhibited; termed DZ50 in *P. falciparum*) and its interaction partner CITH (homolog of worm CAR-I and fly Trailer Hitch), which are responsible for repression of the transcripts encoding the zygote surface antigens P25 and P28 (Mair et al., 2006, 2010). A similar function has been assigned to PUF2 in *P. falciparum*, which also represses a number of female gametocyte transcripts including *p25* and *p28* (Miao et al., 2010; Miao, Wang, et al., 2013).

A yet under-investigated group of RNA-binding proteins are ZFPs with C2H2 (CCHH) and C3H1 (CCCH) motifs. In particular, the C3H1-ZFPs commonly function in RNA-binding with important roles in pre-mRNA splicing, polyadenylation, mRNA export, and translation, as well as ubiquitination and transcriptional repression (reviewed in Ngwa et al., 2021). One of the few C3H1-ZFPs characterized so far is YTH.1, a binding protein of m^6A-modified mRNA in early *P. falciparum* intraerythrocytic parasites that is crucial for post-transcriptional control (Baumgarten et al., 2019). A recent study further identified two *P. falciparum* C3H1-ZFPs, termed PfCZIF1 and PfCZIF2, suggested to assist in regulating the expression of proteins exported into the RBC cytosol after merozoite invasion (Balbin et al., 2023). In addition, a C3H1-ZFP of *P. falciparum* gametocytes, termed ZNF4, was assigned to male gametogenesis. ZNF4-deficient gametocytes are impaired in exflagellation, and comparative transcriptomics demonstrated the downregulation of male-enriched transcripts associated with axonemal dynein complex formation and cell projection organization in parasites lacking ZNF4 (Hanhsen et al., 2022).

The present study aims at investigating the role of the C3H1-ZFP MD3 (male development 3) in gametocyte development and gametogenesis. MD3 was previously identified by us during a transcriptomic

screen for genes deregulated upon treatment of gametocytes with the histone deacetylase (HDAC) inhibitor Trichostatin A (TSA) (Ngwa et al., 2017). Recently, MD3 was also identified as a protein involved in male gametocytogenesis in *P. berghei*, following a global screen of barcoded mutants (Russell et al., 2023). We here show that MD3 is highly expressed in male *P. falciparum* gametocytes and important for male gametocytogenesis. Interactomics demonstrate its involvement in RNA-binding protein complexes, which regulate the expression of sex-specific proteins.

2 | RESULTS

2.1 | MD3 is a C3H1-ZFP predominantly expressed in immature male gametocytes

MD3 (PF3D7_0315600) is a 57-kDa protein with a C3H1-zinc finger domain spanning amino acids 163 to 183 (Figure 1a). It was originally identified in a comparative transcriptomics screen for genes deregulated in immature gametocytes upon TSA treatment, suggesting its epigenetic regulation during gametocyte development (Ngwa et al., 2017). 3D structure prediction of MD3 demonstrated the arrangement of alpha helices and beta strands in the C3H1 domain to coordinate zinc ion binding and domain stabilization (Figure 1b, Figure S1a). An *in silico* principal component analysis (PCA) of single-cell transcriptomes (Malaria Cell Atlas database; Howick et al., 2019) indicated *md3* expression in all asexual and sexual blood stages of *P. falciparum* with high expression specifically in developing gametocytes (Figure S1b–e).

To study the expression profile of MD3 in more detail, we first determined its transcript levels using diagnostic RT-PCR with RNA isolated from different asexual and sexual blood stages of the *P. falciparum* wild-type (WT) strain NF54. We detected high transcript abundance in immature, mature and activated gametocytes, while low transcript levels were detected in rings, trophozoites or schizonts (Figure 1c). Transcript analysis of the housekeeping gene *aldolase* was used as a loading control, and purity of the samples was demonstrated by amplification of transcripts for the asexual blood stage-specific gene *ama1* (apical membrane antigen 1) and for the gametocyte-specific gene *ccp2* (LCCL-domain protein 2). Reverse transcriptase-free cDNA preparations were used to verify that the samples were devoid of gDNA (Figure S2a). These data confirmed transcription of *md3* in gametocytes and are in accord with previous studies (López-Barragán et al., 2011; Ngwa et al., 2017).

We then generated mouse polyclonal antisera against an N-terminal portion of MD3 for protein level analyses (Figure 1a). Lysates from rings, trophozoites, schizonts, immature and mature gametocytes were subjected to Western blot (WB) analysis using the anti-MD3 antisera. Immunoblotting detected MD3 migrating at the expected molecular weight of 57 kDa in lysates of asexual blood stages and gametocytes with high protein levels observed in immature gametocytes (Figure 1d). Antisera against the endoplasmic reticulum-resident protein Pf39 were used as loading control, and lysate from non-infected RBCs (niRBCs) served as negative control.

Subsequent indirect immunofluorescence assays (IFAs) revealed a granular localization of MD3 in the cytoplasm of the *P. falciparum* blood stages. MD3 was detected in roughly 15% and 55% of asexual blood stages and gametocytes, respectively ($n = 100$; see also below), with high protein abundance in immature (stage II and III) gametocytes (Figure 2a). While MD3-positive granules were evenly distributed in rings, trophozoites and schizonts (highlighted by rabbit antisera directed against the 6-cystein protein P92; Sanders et al., 2005), in gametocytes (highlighted by rabbit antisera directed against the 6-cystein protein P230; Williamson et al., 1993), the

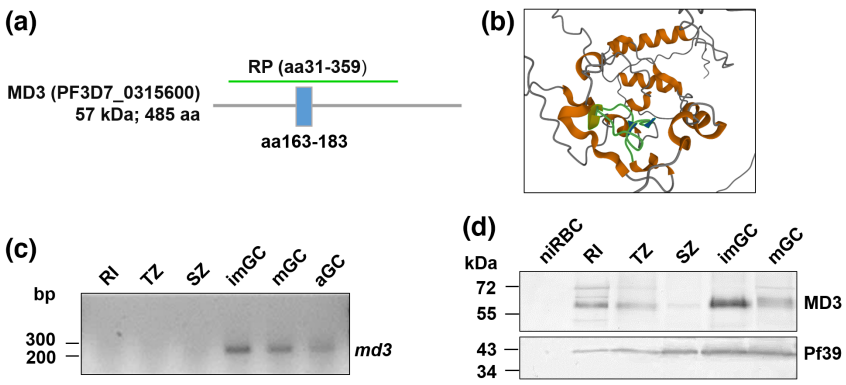

FIGURE 1 Structure of MD3 and expression in the *Plasmodium falciparum* blood stages. (a) Schematic depicting MD3. The region comprising the recombinant protein (RP) is indicated. Blue box, C3H1 domain. (b) Predicted 3D structure of the C3H1 domain of MD3. The 3D predicated structure of the C3H1 zinc finger domain of MD3 is indicated (AlphaFold program). Alpha helices, orange; beta sheets, blue; C3H1 zinc finger domain, green. The full 3D structure is provided in Figure S1 (c) Transcript expression of MD3. Diagnostic RT-PCR was used to amplify *md3* transcript (231 bp) from cDNA generated from total RNA of rings (RI), trophozoites (TR), schizonts (SZ), as well as immature gametocytes (imGC; stages II–IV), mature gametocytes (mGC; stage V) and activated gametocytes (aGC; 30 min post-activation) of WT NF54. Controls are provided in Figure S2a. (d) Protein expression of MD3. Lysates from RI, TZ, SZ, imGC and mGC of WT NF54 were immunoblotted with mouse anti-MD3 antisera to detect MD3 (~57 kDa). Immunoblotting with rabbit antisera against *Pf39* (~39 kDa) served as loading control; lysate of niRBC served as negative control. Results (c, d) are representative of three independent experiments.

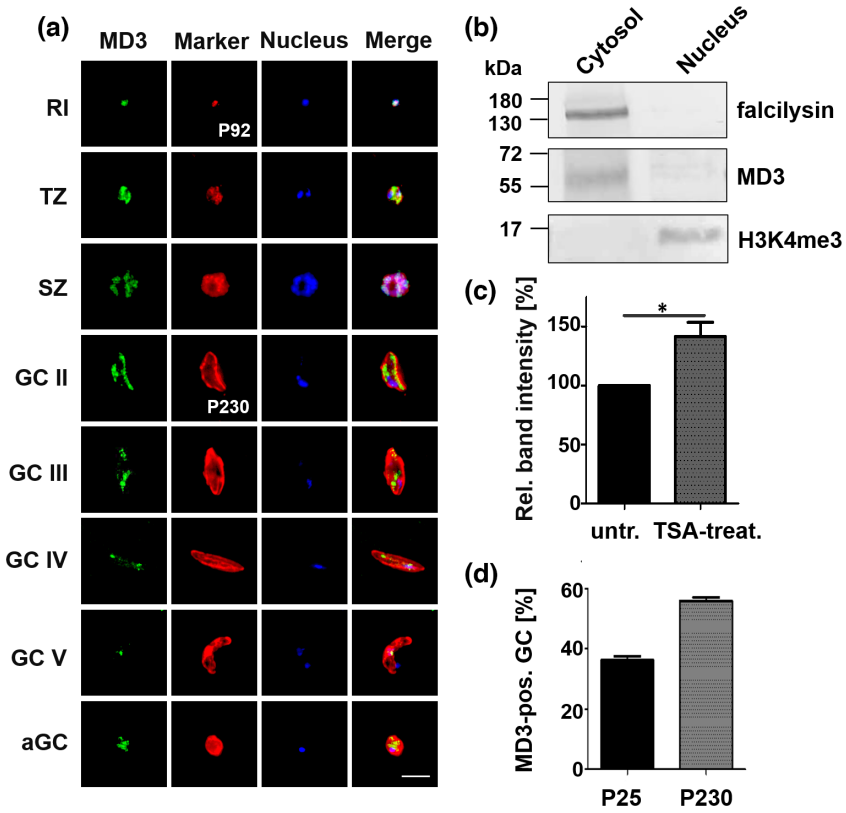

FIGURE 2 Subcellular localization, epigenetic regulation and sex specificity of MD3 in blood stage parasites. (a) Localization of MD3 in the *Plasmodium falciparum* blood stages. Methanol-fixed rings (RI), trophozoites (TZ), schizonts (SZ), gametocyte (GC) stages II–V and activated gametocytes (aGC; 30 min post-activation) were immunolabeled with mouse anti-MD3 antisera (green). Asexual blood stages and gametocytes were highlighted with rabbit antisera directed against P92 and P230, respectively (red); nuclei were highlighted by Hoechst 33342 nuclear stain (blue). Bar, 5 μm. Negative controls are provided in Figure S2b. (b) Subcellular localization of MD3. Cytosolic and nuclear fractions were extracted from immature WT NF54 gametocytes and immunoblotted with mouse anti-MD3 antisera to detect MD3 (~57 kDa). Mouse antisera against the cytosolic protease falcilysin (~138 kDa) and rabbit antisera directed against the histone H3 mark H3K4me3 (~15 kDa) were used to confirm the fraction purity. (c) Quantification of MD3 levels following TSA-treatment. Immature gametocytes were treated with 0.26 μM TSA or 0.5% (v/v) ethanol for control for 24 h. Lysates were immunoblotted with anti-MD3 antisera. MD3 protein levels were evaluated by measuring the band intensities (ImageJ); the values were normalized to the respective *Pf*39 protein band ($n = 4$; mean ± SD; untreated set to 100%). $^*p < 0.05$ (Student's *t*-test). An exemplary immunoblot is provided in Figure S2c. (d) Sex specificity of MD3. Mature WT NF54 gametocytes (GC) were immunolabeled with mouse anti-MD3 antisera and counterlabeled with either rabbit antisera against P230 (expressed in male and female gametocytes) or P25 (expressed in female gametocytes). The percentage of MD3-positive gametocytes was evaluated for 100 gametocytes per marker ($n = 3$; mean ± SD). Results (a, b) are representative of three independent experiments.

granules were located partially near the periphery. In mature and activated gametocytes, the protein levels decreased. For negative control, schizont and gametocytes were immunolabeled with serum from non-immunized mice (Figure S2b).

Subcellular fractionation was conducted using lysates of immature gametocytes to obtain cytosolic and nuclear fractions, which were subjected to WB. MD3 was predominantly found in the cytosolic fraction, while only minor signals were found in the nuclear fraction (Figure 2b). Mouse antisera against the cytosolic protease falcilysin were used as a cytosolic marker, while rabbit antibodies against the histone 3 methylation mark H3K4me3 served as nuclear control.

Because MD3 was originally discovered as a product of a gene transcriptionally upregulated in immature gametocytes that were treated with the epigenetic HDAC inhibitor TSA (Ngwa et al., 2017; see above), we aimed to determine the protein levels of MD3 in dependence of TSA treatment. Lysates of immature gametocytes treated with 0.26 μM TSA for 24 h were harvested and immunoblotted with mouse anti-MD3 antisera, lysates of untreated cultures served as control. Quantitative WB demonstrated a significant increase of MD3 levels to 141% following TSA-treatment compared to untreated controls (set to 100%) (Figure 2c, Figure S2c). These data confirm our previous findings on the increase of MD3 expression upon HDAC inhibition.

Potential sex specificity was determined by IFA as described previously (Bennink et al., 2018). Gametocytes immunolabeling for MD3 were counterlabeled either with rabbit antisera against P230, a protein expressed in both female and male gametocytes (see above), or with rabbit antisera against the female-specific protein P25, and the numbers of MD3-positive gametocytes that counterlabeled for either P230 or P25 were determined. Noteworthy, *P. falciparum* gametocytes usually exhibit a male-to-female sex

ratio of 1:4 (Smith et al., 2000). We showed that approximately 55% of total gametocytes (i.e., P230-positive gametocytes) labeled for MD3, while only 37% of female gametocytes (i.e., P25-positive gametocytes) were MD3-positive (Figure 2d). The results indicate the presence of MD3 in both male and female gametocytes with a higher abundance in males and are in accord with previous reports on high *md3* transcript levels in male gametocytes of *P. falciparum* and *P. berghei* (Lasonder et al., 2016; Russell et al., 2023).

The combined data indicate that MD3 is a cytosolic C3H1-ZFP particularly present in male immature gametocytes, the expression of which is linked to HDAC-mediated epigenetic regulation.

2.2 | MD3 deficiency results in impaired intraerythrocytic growth, delayed gametocyte maturation and aborted exflagellation

For functional characterization of MD3, we generated line MD3-HA-*glmS*, using vector pSLI-HA-*glmS* (Figure S3a; Birnbaum et al., 2017), which enables conditional *md3* transcript knockdown upon addition of glucosamine (GlcN). Successful vector integration into the targeted *md3* locus was shown by diagnostic PCR (Figure S3b). The MD3-HA-*glmS* line was free of WT parasites.

First, the MD3-HA-*glmS* line was used to confirm the above protein expression data. WB analysis using rat anti-HA antibody confirmed peak expression in immature gametocytes and detected MD3-HA primarily in the cytosolic fraction (Figure S4a,b). In addition, MD3-HA expression in immature gametocytes was upregulated to 135%, when these were treated with TSA (Figure S4c,d). IFAs localized MD3-HA in cytoplasmic granules of the asexual blood stages and gametocytes, while no MD3-HA labeling was detected in the WT NF54 blood stages (Figure S5a). Approximately 59% of total gametocytes (i.e., P230-positive gametocytes) and 43% of female gametocytes (i.e., P25-positive gametocytes) were MD3-HA-positive (Figure S5b,c), confirming prominent MD3-HA expression in male gametocytes.

Subsequently, the MD3-HA-*glmS* line was used for loss-of-function phenotyping. Treatment of the asexual blood stages of line MD3-HA-*glmS* with 5 mM GlcN for 72 h reduced the MD3-HA protein levels to 63% compared to untreated cultures, as demonstrated by quantitative WB (Figure S6a,b). In the following, tightly synchronized ring stages of line MD3-HA-*glmS* with an initial parasitemia of 0.25% were cultivated with GlcN and the parasitemia was evaluated by Giemsa-stained thin blood smears every 24 h over a period of 96 h. Untreated cultures of line MD3-HA-*glmS* as well as GlcN-treated and untreated WT NF54 were carried along for controls. The intraerythrocytic growth assay revealed a significant reduction in the parasitemia of GlcN-treated MD3-HA-*glmS* at 96 h as compared to the controls, indicating that the knockdown of *md3-ha* transcript impairs asexual blood stage development (Figure 3a). However, no morphological abnormalities were observed in the GlcN-treated blood stage parasites compared to the controls (Figure S6c). Further, no stage conversion shifts were recorded, when the numbers of ring stages, trophozoites and schizonts were evaluated (Figure S7a).

In order to determine the effect of MD3-HA deficiency on gametocytogenesis, tightly synchronized ring stage cultures of line MD3-HA-*glmS* were induced to form gametocytes by addition of lysed RBCs for 24 h. After induction, cultures were maintained in cell culture medium supplemented with 20 U/mL heparin sulfate to kill the asexual blood stages for 4 days and with GlcN for transcript knockdown till day 13. Samples were taken every 48 h starting from day 3 after induction and subjected to Giemsa staining. The gametocytemia was evaluated and the numbers of stage II to V gametocytes were determined microscopically. The gametocytemia was not affected in the GlcN-treated MD3-HA-*glmS* line as compared to untreated transgenic parasites or GlcN-treated and untreated WT NF54 (Figure 3b). However, a delay in gametocyte maturation from stage IV to stage V was observed in the MD3-HA-*glmS* line at day 13 of GlcN treatment compared to controls (Figure 3c, Figure S7b). Giemsa staining, though, did not reveal any morphological differences in the GlcN-treated MD3-HA-*glmS* gametocytes (Figure S6c).

In a next step, the effect of MD3-HA deficiency was studied during male gametogenesis. Highly synchronized ring stage cultures of line MD3-HA-*glmS* were induced to form gametocytes. Between day 7 and 11 post-induction, the MD3-HA-*glmS* gametocytes were treated with GlcN for transcript knockdown and then allowed to recover for 2 days to avoid impairment of gametogenesis by GlcN. Untreated cultures of line MD3-HA-*glmS* as well as GlcN-treated and untreated WT NF54 were carried along for control. Exflagellation of male gametocytes was determined on days 13 and 15 post-induction by microscopy. Following gametocyte activation, the number of exflagellation centers was counted and the results were adjusted to the numbers of mature gametocytes as evaluated prior to activation by Giemsa staining (Figure S8a). On day 13 post-induction, a significant reduction in the relative numbers of exflagellation centers was observed for line MD3-HA-*glmS* treated with GlcN compared to the controls (Figure 3d). No significant difference in the relative numbers of exflagellation centers, though, was observed on day 15 post-induction (Figure S8b).

We then investigated the potential effect of MD3 deficiency on sex ratio shifting. Highly synchronized schizont stage cultures of line MD3-HA-*glmS* were treated with GlcN for 72 h before gametocyte induction and the treatment was continued until day 9 post-induction. As a control, untreated cultures of line MD3-HA-*glmS* and GlcN-treated and untreated WT NF54 were used. IFAs were carried out on day 9 post-induction, using antisera against P230 and P25. On day 9 post-induction, the numbers of female gametocytes (i.e., gametocytes positive for P25 and P230) and male gametocytes (i.e., gametocytes negative for P25 and positive for P230) were evaluated (Figure S9a,b). A significant increase in the number of female gametocytes was observed in the GlcN-treated MD3-HA-*glmS* line as compared to the controls.

The combined phenotyping data indicate that MD3 is crucial for both intraerythrocytic development and gametocyte maturation with a particular impact on male gametocytogenesis and in consequence exflagellation.

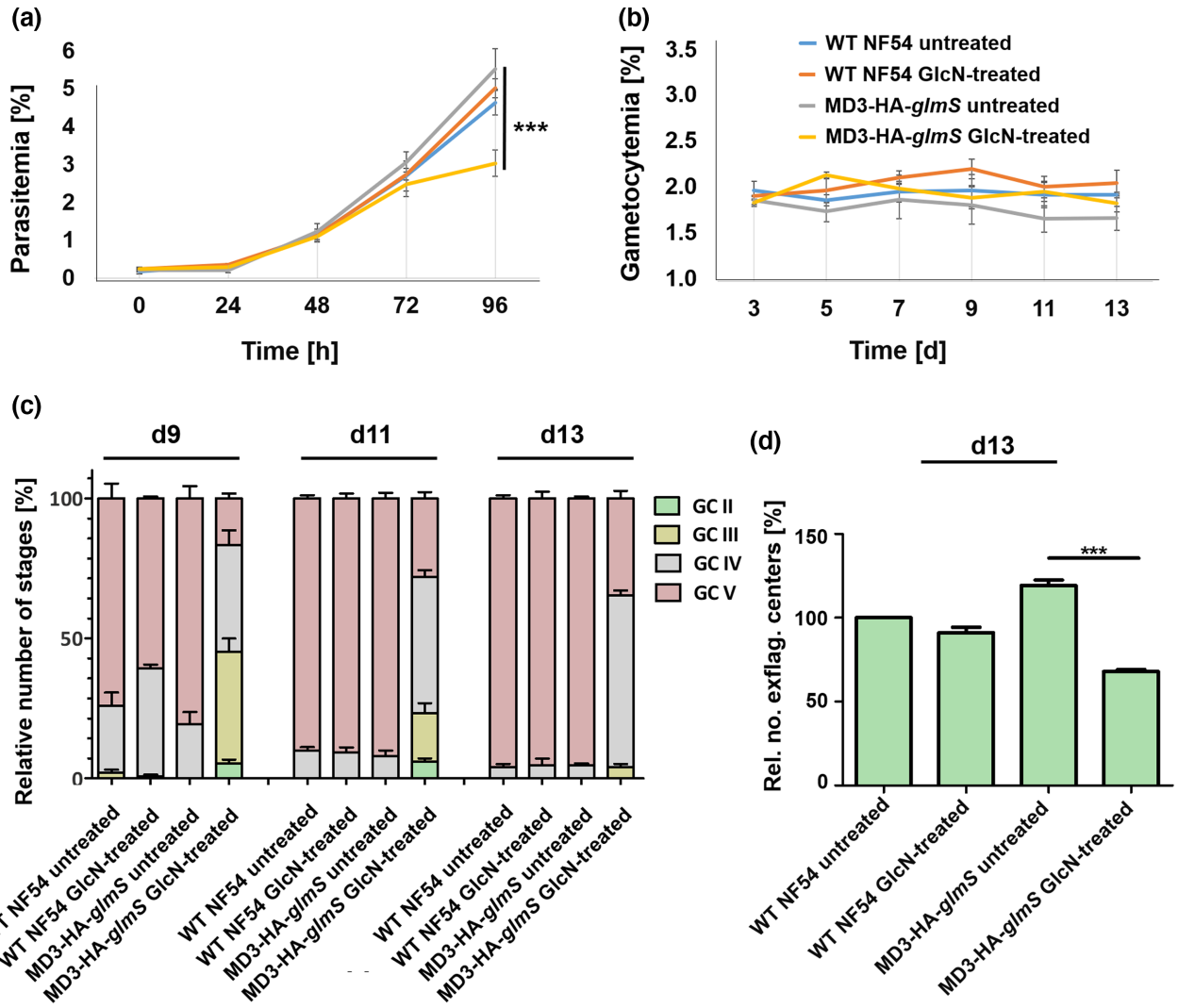

FIGURE 3 The effect of MD3-HA deficiency on intraerythrocytic growth and gametocyte development. (a) Asexual blood stage replication following *md3-ha* knockdown. Synchronized ring stage cultures of WT NF54 and line MD3-HA-*glmS* with a starting parasitemia of 0.25% were maintained in cell culture medium supplemented or not with 5 mM GlcN. The parasitemia was followed via Giemsa smears at 0–96 h post-seeding ($n = 3$; mean ± SD). ***$p < 0.001$ (One-way ANOVA with post hoc Bonferroni multiple comparison test). (b) Gametocyte development following *md3-ha* knockdown. Synchronized ring stage cultures of line MD3-HA-*glmS* and WT NF54 at a final parasitemia of 7.5% were induced and maintained in cell culture medium supplemented or not with GlcN. The gametocytemia was followed via Giemsa smears at day 3–13 post-induction ($n = 3$; mean ± SD). (c) Gametocyte maturation following *md3-ha* knockdown. Relative numbers of gametocyte stages II–V as described in (b) were followed via Giemsa smears in 50 iRBCs at days 3–13 ($n = 3$; mean ± SD). The complete assay is shown in Figure S7b. (d) Effect of *md3-ha* knockdown on exflagellation. Synchronized ring stage cultures of line MD3-HA-*glmS* and WT NF54 at a final parasitemia of 7.5% were induced. The cultures were treated with 50 mM GlcNac for 2 days and 20 U/mL heparin sulfate for the next 2 days and then maintained in normal cell culture medium. On day 7–10 post-induction, the gametocytes were maintained in cell culture medium supplemented or not with GlcN. On day 13, gametocytes were activated and the numbers of exflagellation centers were evaluated ($n = 3$; mean ± SD; WT NF54 untreated set to 100%). ***$p < 0.001$ (One-way ANOVA with post hoc Bonfferoni multiple comparison test). Exemplary images of mature gametocytes used in the exflagellation assays on day 13 are provided in Figure S8a.

2.3 | The MD3 interaction network is composed of regulators of sexual development

To determine the MD3 interaction network, we generated transgenic lines episomally expressing an MD3-GFP-BirA fusion protein as described (Musabyimana et al., 2022; Sassmannshausen et al., 2023). Blood stage parasites were transfected with the vectors pARL-MD3-*pfama1*-GFP-BirA or pARL-MD3-*pffnpa*-GFP-BirA, whereby the expression of MD3-GFP-BirA was either controlled by the asexual blood stage-specific *pfama1* or the gametocyte-specific *pffnpa* promotor (Figure S10a,b). Diagnostic PCR confirmed the presence of the respective vectors in the transgenic lines (Figure S10c,d).

WB analysis, using mouse anti-GFP antibody, demonstrated the expression of the MD3-GFP-BirA fusion protein in lysates from asexual blood stages and gametocytes of lines MD3-*pfama1*-GFP-BirA

and MD3-*pffnpa*-GFP-BirA, respectively. In the transgenic lines, MD3-GFP-BirA could be detected at the expected molecular weight of approximately 118 kDa (Figure 4a). In addition, immunolabeling confirmed the cytoplasmic localization of MD3-GFP-BirA in trophozoites and gametocytes of the respective lines (Figure 4b).

Subsequently, lysates were prepared from asexual blood stages and gametocytes of lines MD3-*pfama1*-GFP-BirA and MD3-*pffnpa*-GFP-BirA, respectively, which were incubated with 50 µM biotin for 24 h. Immunoblotting, using alkaline phosphatase-conjugated streptavidin, led to the detection of multiple protein bands in both lysates, indicative of biotinylated proteins, including a protein of approximately 118 kDa representing biotinylated MD3 (Figure 4c). Furthermore, immunolabeling with fluorophore-conjugated streptavidin showed the presence of biotinylated proteins in the cytoplasm of biotin-treated trophozoites and gametocytes of the respective transgenic lines, respectively (Figure S10e). WT NF54 parasites served as negative controls in the experiments.

Lines MD3-*pfama1*-GFP-BirA and MD3-*pffnpa*-GFP-BirA were subjected to mass spectrometry-based proximity-dependent biotin identification (BioID-MS) to identify the MD3 interactome. Schizonts and immature gametocytes of the respective lines were treated with 50 µM biotin for 24 h and equal amounts of parasites were harvested. Three independent samples were collected per line and mass spectrometric analysis was performed on streptavidin-purified protein samples with three technical replicas for each sample; WT NF54 samples were used as a negative control. BioID-MS resulted in the identification of 41 significantly enriched hits in the asexual blood stages of line MD3-*pfama1*-GFP-BirA (after exclusion of proteins with a signal peptide) and 98 significantly enriched hits in gametocytes of line

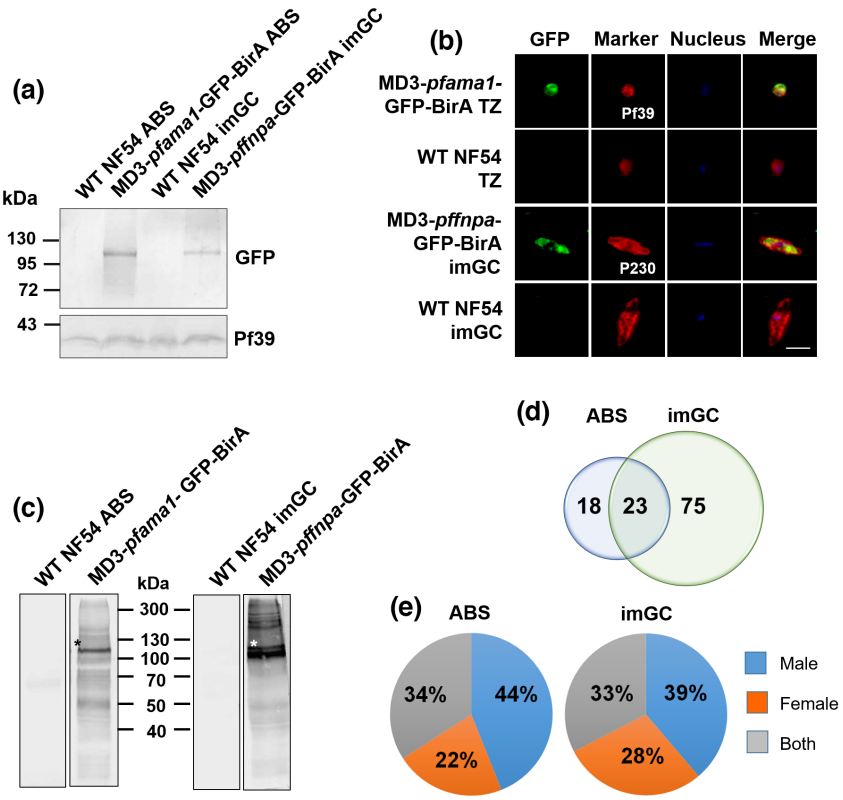

FIGURE 4 Verification of the MD3-GFP-BirA parasite lines to be used in BioID. (a) Verification of MD3-GFP-BirA expression. Lysates of mixed asexual blood stages (ABS) of line MD3-*pfama1*-GFP-BirA and purified immature gametocytes (imGC) of line MD3-*pffnpa*-GFP-BirA were immunoblotted with mouse anti-GFP antibody to detect MD3-GFP-BirA (~118 kDa). Immunoblotting with rabbit antisera against *Pf*39 (~39 kDa) served as loading control; lysate of WT NF54 served as negative control. (b) Localization of MD3-GFP-BirA in blood stage parasites. Methanol-fixed trophozoites (TZ) of line MD3-*pfama1*-GFP-BirA and immature gametocytes (imGC) of line MD3-*pffnpa*-GFP-BirA were immunolabeled with mouse anti-GFP antibody to detect MD3-GFP-BirA (green). Trophozoites were counterlabeled with rabbit anti-*Pf*39 antibody and gametocytes with rabbit anti-P230 antisera (red); nuclei were highlighted by Hoechst 33342 nuclear stain (blue). WT NF54 served as control. Bar, 5 µm. (c) Detection of biotinylated proteins in the MD3-GFP-BirA lines. Asexual blood stages (ABS) of line MD3-*pfama1*-GFP-BirA and immature gametocytes (imGC) of line MD3-*pffnpa*-GFP-BirA were treated with 50 µM biotin for 24 h. Lysates were immunoblotted with streptavidin coupled to alkaline phosphatase. Asterisks indicate biotinylated MD3. Biotin-treated WT NF54 served as negative control. (d) Venn diagram depicting the MD3 interactors grouped by blood stage. Asexual blood stages (ABS) and immature gametocytes (imGC) were treated with biotin as described above and streptavidin bead-purified biotinylated proteins were subjected to BioID-MS. Hits with predicted signal peptides were excluded from further analysis. A total of 116 interactors were identified and grouped by blood stage. (e) Pie chart depicting the MD3 interactors (percentage of total numbers) grouped by sex (PlasmoDB). Results (a–c) are representative of three independent experiments. Detailed information on the interactors is provided in Tables S1 and S2.

MD3-*pffnpa*-GFP-BirA compared to WT NF54 control (Figure 4d; Tables S1 and S2). A total of 23 proteins was found in both lines, which included the bait protein MD3.

In silico transcript analyses (according to table "Transcriptomes of 7 sexual and asexual life stages"; López-Barragán et al., 2011; see PlasmoDB database; Aurrecoechea et al., 2009) showed that the majority of the 98 MD3 interactors identified in line MD3-*pffnpa*-GFP-BirA exhibited peak expression in ookinetes and mature gametocytes in addition to ring stages and trophozoites, while most of the 41 MD3 interactors identified in the MD3-*pfama1*-GFP-BirA line had peak expression in ring stages and early trophozoites (Figure S11a,b). When the sex specificity of the interactors was evaluated (according to table "Gametocyte transcriptomes"; Lasonder et al., 2016; see PlasmoDB database; Aurrecoechea et al., 2009), roughly 40% of the MD3 interactors of immature gametocytes and asexual blood stages could be assigned to the male sex (Figure 4e).

Gene Ontology (GO) enrichment analysis (Ge et al., 2020) of the 98 MD3 interactors of immature gametocytes revealed their association with biological processes such as translation, post-transcriptional regulation of gene expression and macromolecule metabolic processes (Figure 5a). The interactors were primarily assigned to the cytoplasm and had associations with ribosomes and mRNP complexes, e.g., the eukaryotic translation initiation factor 4F complex, the CCR4-NOT complex and P-bodies (Figure 5b). Molecular functions included mRNA- and rRNA-binding as well as binding to heterocyclic and organic cyclic compounds (Figure 5c). The 41 interactors of asexual blood stages were assigned to biological processes such as translation and gene expression with cellular component associations to the cytoplasm and mRNP complexes, while mRNA-binding, rRNA-binding as well as organic cyclic compound binding represented the enriched terms for molecular functions (Figure S12a–c).

The putative MD3 interactors were further subjected to STRING-based analyses to investigate the protein–protein interaction networks (Szklarczyk et al., 2019). The MD3 interactome of immature gametocytes comprised four defined clusters, the most comprehensive of which included multiple ribosomal proteins (Figure 6, cluster A; Table S3). A similar cluster was identified for the MD3 interactors in the asexual blood stages (Figure S13; Table S4). Three more clusters of MD3 interactors in immature gametocytes (clusters B-D) were tightly linked to processes of transcription and translation. Cluster B comprised 15 proteins associated to post-transcription and translation, e.g., NOT family proteins, eukaryotic translation initiation factors or RNA-binding proteins, while cluster C included five proteins predicted to be located in the nucleus, including an NPL domain protein and an NTF2 domain protein of unknown functions (Figure 6; Table S3). Cluster D was formed by seven proteins linked to translational control, e.g., the RNA-binding proteins PUF1 and ALBA3 or the translational repressor CITH (Banerjee et al., 2023; Bunnik et al., 2016; Mair et al., 2010; Shrestha et al., 2016). The most interesting cluster of the STRING analysis was cluster E that comprised nine proteins as well as various satellite proteins. The majority of these proteins had recently been linked to the development of male and female gametocytes, e.g., the cluster proteins GD1, FD1, FD2, MD2, MDV1 and the satellite proteins FD4, MD1, MD3, ZNF4 and RNF1 (Furuya et al., 2005; Gomes et al., 2022; Hanhsen et al., 2022; Ngwa et al., 2017; Russell et al., 2023).

The combined BioID-MS results unveiled an important interaction network of MD3 with proteins related to post-transcriptional and translational control in immature gametocytes and highlighted a striking interaction of MD3 with other RNA-binding proteins, including various ZFPs, involved in the regulation of gametocyte development.

2.4 | MD3 forms protein complexes with RNA-binding proteins

In a final set of experiments, we investigated in more detail the interaction of MD3 and select RNA-binding proteins as identified by BioID-MS, using co-immunoprecipitation assays. We made use of the previously published ZNF4-HA-*glmS* line (Hanhsen et al., 2022). In addition, we generated a parasite line expressing PUF1 fused to an HA-tag, using the pSLI-HA-*glmS* vector as described above. Successful vector integration into the targeted *puf1* locus was shown by diagnostic PCR (Figure S14a). Expression of HA-tagged PUF1 was subsequently shown by WB analysis using rat anti-HA antibody. Immunoblotting highlighted a protein band running at the expected molecular weight of ~227 kDa in the lysates of asexual blood stages and immature gametocytes of PUF1-HA-*glmS* parasites, while no band was visible in the WT NF54 control (Figure S14b).

For the co-immunoprecipitation assays, lysates were generated from immature gametocytes of lines MD3-HA-*glmS*, PUF1-HA-*glmS*, and ZNF4-HA-*glmS*; WT NF54 lysate was used as a control. The bait proteins were precipitated with protein-G bead-bound rabbit anti-HA or rat anti-HA antibodies and precipitated proteins were subjected to WB analysis. In immunoprecipitates of line MD3-HA-*glmS*, protein bands representing RNF1, CITH, and the polyadenylate-binding protein PABP1 could be detected running at the expected molecular weights, following immunoblotting with the respective mouse or rabbit antibodies (Figure 7a,b). When immunoprecipitates of lines ZNF4-HA-*glmS* and PUF1-HA-*glmS* were subjected to WB analysis, MD3 could be detected using the respective mouse antibody (Figure 7c,d). The precipitation of the respective bait protein was confirmed by immunoblotting with rat anti-HA antibody; immunoblotting with rabbit anti-*Pf39* antibody was used as a negative control. In addition, WT NF54 was subjected to co-immunoprecipitation assays and no bands for precipitated parasite proteins were visible (Figure S15a–d).

In conclusion, the co-immunoprecipitation data confirmed protein–protein interactions between MD3 and selected RNA-binding proteins of immature gametocytes.

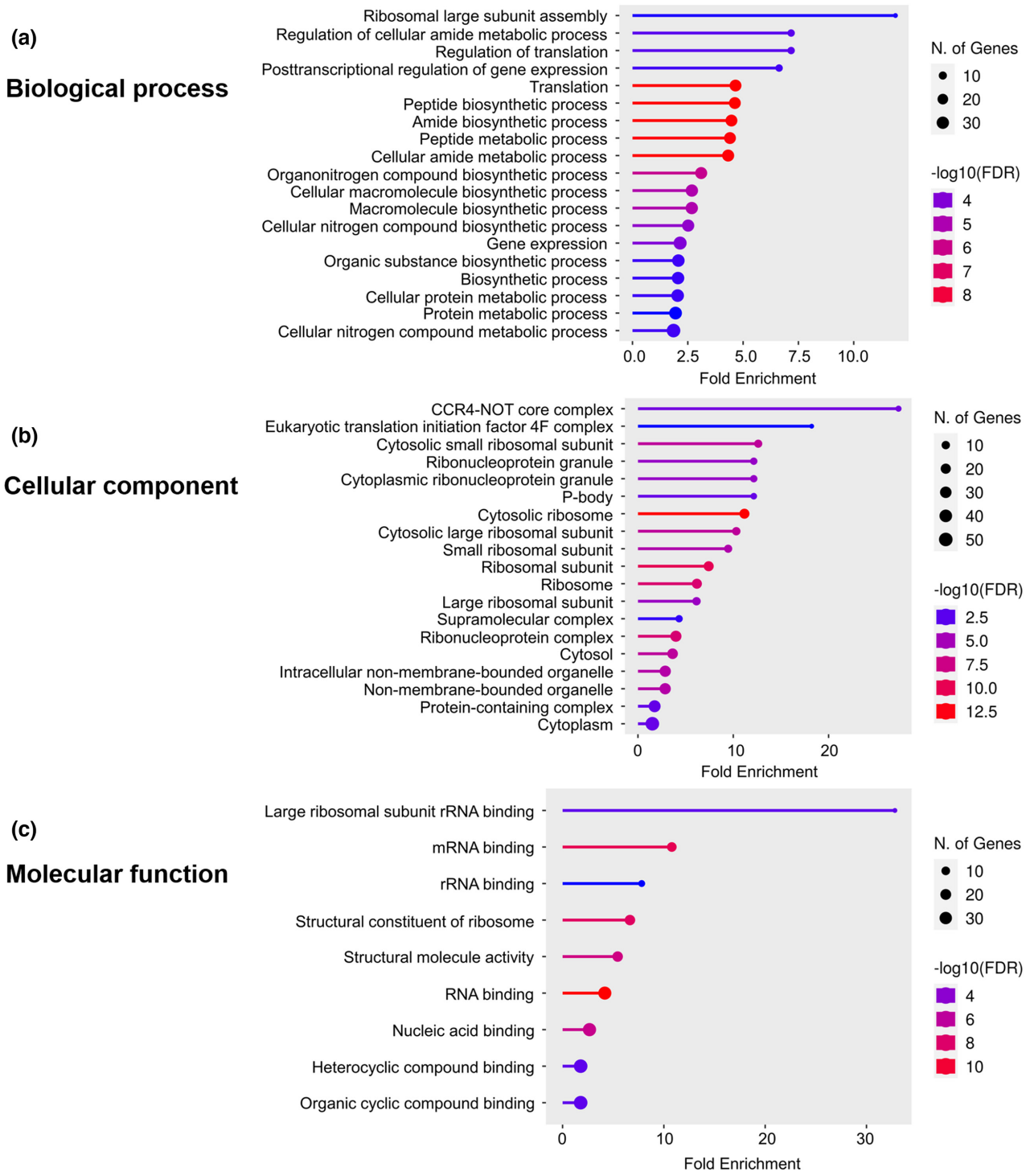

FIGURE 5 Functional prediction of MD3 interactors in immature gametocytes. GO enrichment analysis of the 98 putative MD3 interactors in immature gametocytes was performed to display the enriched GO terms (ShinyGO 0.77; $p < 0.05$) based on biological process (a), cellular component (b) and molecular function (c).

3 | DISCUSSION

Gametocytogenesis of malaria parasites requires a tight control of transcriptional and translational regulation, and RNA-binding proteins play crucial roles during this process. In this study, we report on the importance of the C3H1-ZFP MD3 in regulating male gametogenesis of *P. falciparum* by interacting with RNA-binding proteins. We show that MD3 associates with granules in the cytoplasm of asexual and sexual blood stages with peak protein levels in immature male gametocytes. We also confirmed the dependence of MD3 expression on HDAC-mediated epigenetic regulation with inhibition of HDAC activity resulting in higher MD3 levels.

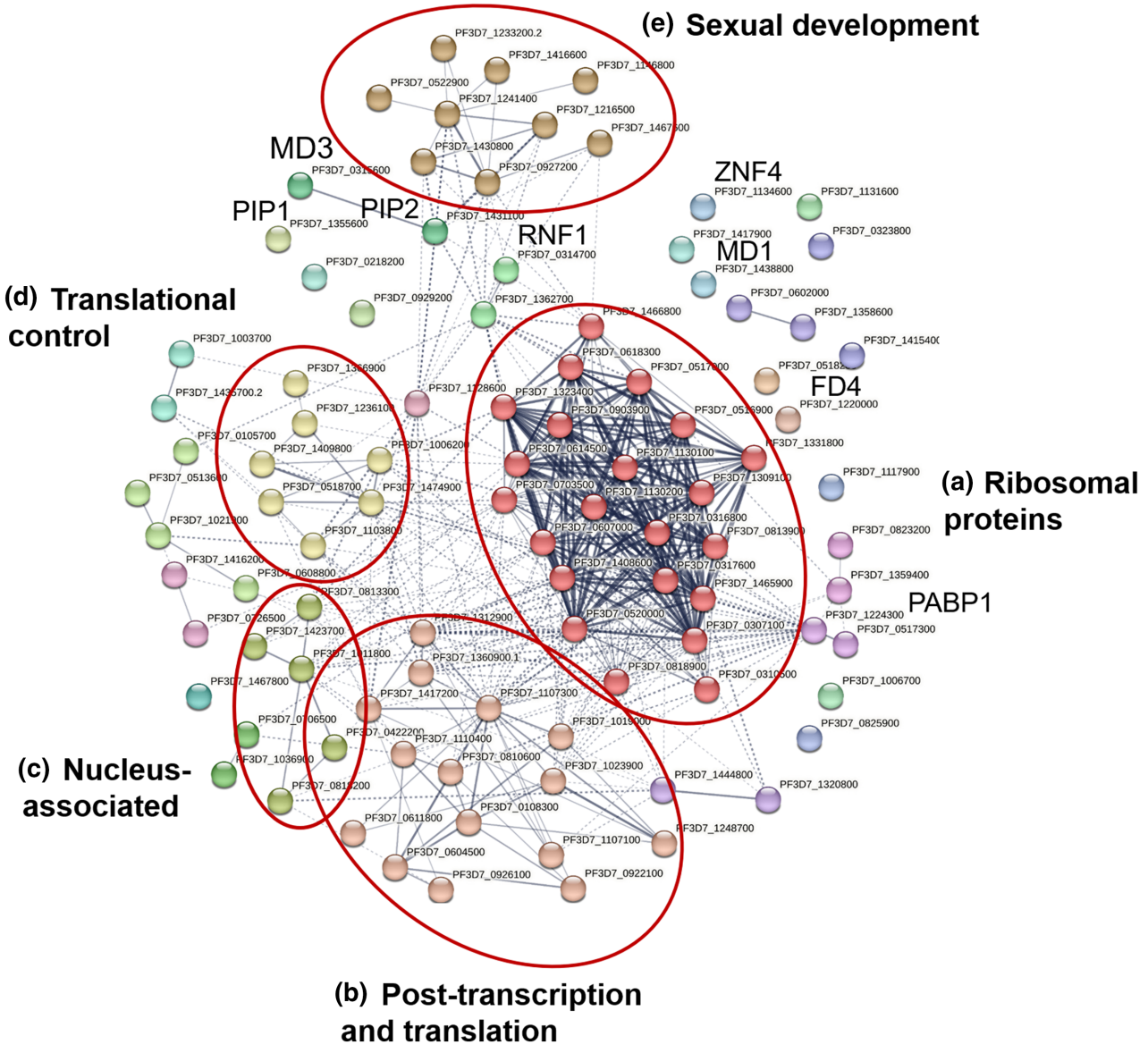

FIGURE 6 Network analysis of the MD3 interactors in immature gametocytes. A protein–protein network analysis of the 98 putative MD3 interactors in immature gametocytes was performed (STRING; medium interaction confidence of 0.4). Line thickness specifies the strength of data support between the proteins. Clustering of the interactors was employed by the Markov Clustering (MCL) algorithm with an inflation parameter of 3; dotted lines represent the connection among the hits of different clusters. On the basis of physical interactions among the query proteins, five main clusters were identified, i.e. (A) ribosomal proteins, (B) post-transcription and translation, (C) nucleus-associated, (D) translational control, and (E) sexual development. Detailed information on each cluster and its components is provided in Table S3.

Further, MD3 deficiencies affect intraerythrocytic replication and particular impair maturation of male gametocytes, which in consequence affects exflagellation. Noteworthy, previous transcriptomics analyses indicated peak expression of MD3 in ookinetes (López-Barragán et al., 2011), suggesting an additional role of MD3 in these stages.

To unveil the MD3 interactome in asexual and sexual blood stage parasites, we employed BioID-MS analyses, using vectors pARL-MD3-*pfama1*-GFP-BirA or pARL-MD3-*pffnpa*-GFP-BirA. While these vectors were previously successfully used for BioID analyses (Musabyimana et al., 2022; Sassmannshausen et al., 2023), it should be noted that *pffnpa*, the promotor of which was used to drive episomal MD3-GFP-BirA overexpression in gametocytes, is highly expressed in females (e.g., Lasonder et al., 2016; Scholz et al., 2008). The use of heterologous promoters in overexpression plasmids may in general affect the outcome of interactome analyses, in particular, when studying differential protein levels during male versus female gametocytogenesis.

BioID-MS identified 41 putative MD3 interactors in the asexual blood stages and 98 interactors in immature gametocytes; 23 proteins were shared by both stages. In-depth bioinformatic analyses demonstrated a strong link of these interactors with various RNA-binding complexes like the CCR4-NOT complex, the eukaryotic

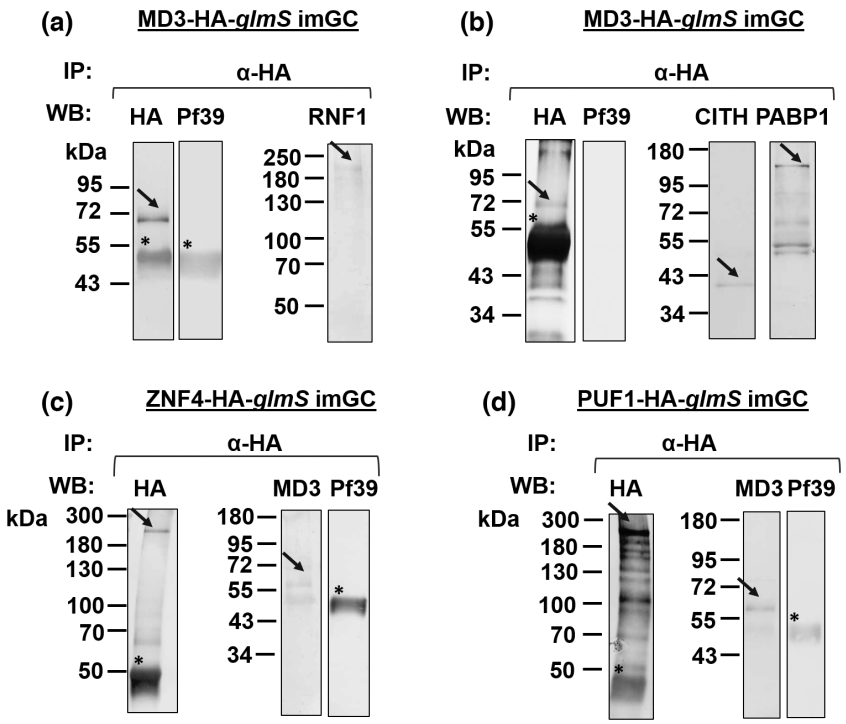

FIGURE 7 Protein interactions of MD3 with RNA-binding proteins. Lysates of immature gametocytes (imGC) of lines MD3-HA-*glmS* (a, b), ZNF4-HA-*glmS* (c), and PUF1-HA-*glmS* (d) were subjected to co-immunoprecipitation assays. Protein complexes were immunoprecipitated using polyclonal rabbit or rat anti-HA antibodies, followed by immunoblotting with rabbit or rat anti-HA antibodies, mouse anti-RNF1 antisera, rabbit anti-CITH antibody, rabbit anti-PABP1 antibody or mouse anti-MD3 antisera to detect the precipitated proteins (arrows; MD3-HA, ~60 kDa; ZNF4-HA, ~207 kDa, PUF1-HA, ~227 kDa; RNF1, ~138 kDa, MD3, ~57 kDa, CITH, ~39 kDa, PABP1, ~97 kDa). Immunoblotting with rabbit anti-*Pf*39 (~39 kDa) served as negative control. Asterisks signify bands corresponding to the heavy chains of the precipitation antibody. Results are representative of two to three independent experiments.

translation initiation complex, mRNP complexes and P-bodies/stress granules in addition to ribosomal proteins suggesting the involvement of MD3 in the regulation of mRNA processing and translation (selected interactors are summarized in Table 1). STRING analyses confirmed these interactions by highlighting four distinct clusters in immature gametocytes, i.e., the post-transcription and translation cluster (cluster B), a nucleus-associated protein cluster (cluster C), the translational control cluster (cluster D), and a cluster comprising RNA-binding proteins recently linked to regulating sexual development (cluster E), in addition to a ribosome-related cluster that was also found in the interactome of the asexual blood stages (cluster A).

Clusters A-D lie in close proximity to each other and are thematically linked. Here found are proteins of the CCR4-NOT and the eukaryotic translation initiation complexes as well as RNA-binding proteins. Some of the most prominent interactors of MD3 include known activators of translation, e.g., PABP, PAIP and eIF4G. For example, the translation initiation factor eIF4G (together with eIF4A and eIF4E) is linked to the mRNA 5′-cap and interacts with PABP and PAIP1 to facilitate mRNA pseudo-circularization and hence transcript stabilization. Interestingly, in *P. falciparum*, the DHH1/DDX6-like RNA helicase DOZI has been identified as a potential eIF4A protein and shown to interact with eIF4E (Tarique et al., 2013). Noteworthy, the PABP-mediated mRNA closed-loop can also facilitate transcript destabilization by providing the physical contact between mRNA-binding proteins, which typically target the 3′-UTR (untranslated region), and the 5′-UTR of the transcript in order to suppress translation (reviewed in Bennink & Pradel, 2019).

MD3 further interacts with components important for transcript decay, like the NOT proteins of the CCR4-NOT deadenylase complex that contribute to poly(A) tail-shortening. Importantly, one of the MD3 interactors, NOT1-G, has been described as a regulator of sexual stage maturation in *P. yoelii*. NOT1-G localizes to cytoplasmic granules in gametocytes and its deficiencies lead to defects in the formation of male gametes as well as of zygotes (Hart et al., 2021). Relevant to this, CCR4-1 was also reported to be crucial for the development and activation of male *P. yoelii* gametocytes as genetic disruption or catalytic inactivation of CCR4-1 results in defective male gametocyte maturation and hence, parasite transmission (Hart et al., 2019).

A variety of RNA-binding proteins mediate the interaction between the CCR4-NOT complex and the 3′-UTR, including PUF proteins, which can increase decapping and deadenylation, or the decapping DDH1/DDX6 activator that associates with Not1, and most of these factors are conserved in *P. falciparum* (reviewed in Bennink & Pradel, 2019). Importantly, some of the transcript decay factors were identified as interactors of MD3, like PUF1, which contributes to the maintenance and differentiation of *P. falciparum* gametocytes, with lack of PUF1 leading to a sharp decline in the late stage

TABLE 1 Selected interactors of *Plasmodium falciparum* MD3.

GeneID	Short name	Name	*P. berghei* ortholog/*P. yoelii* ortholog	Cluster	Function	References
PF3D7_0518700	PUF1	mRNA-binding protein PUF1	PBANKA_1233500/PY17X_1236900	D	Differentiation and maintenance of gametocytes in *P. falciparum*	Shrestha et al. (2016)
PF3D7_0927200	GD1	gametocyte development protein GD1	PBANKA_0828000/PY17X_0831300	E	Female fate determination and male differentiation in *P. berghei*	Russell et al. (2023)
PF3D7_1103800	NOT1-G	CCR4-NOT transcription complex subunit NOT1-G	PBANKA_1025500/PY17X_1027900	D	Male and female gametogenesis in *P. yoelii*	Hart et al. (2021)
PF3D7_1134600	ZNF4	CCCH-type zinc finger protein ZNF4	Ortholog of *P. berghei* GD1 according to (Russell et al., 2023)	E	Male gametogenesis in *P. falciparum*	Hanhsen et al. (2022)
PF3D7_1146800	FD2	Female development protein FD2	PBANKA_0902300/N/A	E	Female differentiation in *P. berghei*	Russell et al. (2023)
PF3D7_1216500	MDV1	Male development gene 1	PBANKA_1432200/PY17X_1434500	E	Male sexual development in *P. falciparum*; gametogenesis in *P. berghei*	Lal et al. (2009), Ponzi et al. (2009), Furuya et al. (2005) and Xu et al. (2021)
PF3D7_1220000	FD4	Female development protein FD4	PBANKA_1435200/PY17X_1437600	E satellite	Female differentiation in *P. berghei*	Russell et al. (2023)
PF3D7_1233200	MD2	Male development protein MD2	PBANKA_1447900/PY17X_1450400	E	Male fate determination in *P. berghei*	Russell et al. (2023)
PF3D7_1241400	FD1	Female development protein FD1	PBANKA_1454800	E	Female differentiation in *P. berghei*	Russell et al. (2023)
PF3D7_1355600	PIP1	PhIL1 interacting protein PIP1	N/A	E satellite	Maturation of gametocytes in *P. falciparum*	Parkyn Schneider et al. (2017)
PF3D7_1438800	MD1	Male development protein MD1	PBANKA_1302700/PY17X_1306500	E	Male fate determination and development in *P. falciparum* and *P. berghei*	Gomes et al. (2022) and Russell et al. (2023)
PF3D7_1474900	CITH	Trailer hitch homolog	PBANKA_1301300/PY17X_1304900	D	Translational repression in female gametocytes in *P. berghei*	Mair et al. (2010)

gametocytes and a sex-ratio shift to males (Shrestha et al., 2016). In *P. falciparum*, two more members of the PUF family are known, PUF2 and PUF3. While PUF3 was reported to participate in ribosome biogenesis, *puf2* gene knockout promotes the formation particularly of male *P. falciparum* gametocytes (Miao et al., 2010). Moreover, PUF2 binds the transcripts of P25 and P28 via PUF-binding elements in their 3´-UTR, thereby contributing to the translational repression of these transcripts (Miao, Fan, et al., 2013).

Of particular importance is the interaction of MD3 with CITH, a master regulator of translational repression in female gametocytes (reviewed in Bennink et al., 2016; Bennink & Pradel, 2019). CITH was previously shown to interact with DOZI and together they repress mRNA encoding P25 and P28 in female *P. berghei* gametocytes (Mair et al., 2006, 2010). Characterization of DOZI- and CITH-associated proteins identified various interactors typical for stress granule components and translational regulation like eukaryotic translation initiation factors or PABP proteins as well as the DNA/RNA-binding proteins ALBA1-4 (Chene et al., 2012; Mair et al., 2010). The ALBA proteins ALBA1 and ALBA4 were previously linked to mRNA homeostasis and translational regulation, while ALBA3, which was here identified as an interactor of MD3, has recently been reported to have nuclease activity (Banerjee et al., 2023; Munoz et al., 2017; Vembar et al., 2015). Noteworthy, we confirmed the binding of MD3 to CITH and PUF1 by co-immunoprecipitation assays. The combined protein interaction network analyses of clusters A-D let us conclude that MD3 has important roles in protein biosynthesis by interacting with both activators and repressors of translation.

The most striking protein network is depicted in cluster E, which demonstrates the interaction of MD3 with regulators of sexual development as recently identified by Russell et al. (2023). In this study, a genetic screen of barcode mutants identified a set of 10 genes with roles in male and female determination in *P. berghei*. MD3 was one of three identified ZFPs and its role in sexual development was highlighted. For instance, the disruption of the *md3* gene in *P. berghei* resulted in a marked sex ratio shift towards females, with few fertile males, signifying its importance in male gametocytogenesis (Russell et al., 2023). Interestingly, we witnessed six orthologs of the 10 gametocyte development regulators of *P. berghei* in the MD3 interactome of immature *P. falciparum* gametocytes, i.e., the male development proteins MD1 and MD2, the gametocyte development protein GD1, and the female development proteins FD1, FD2 and FD4.

Best investigated in the study by Russell et al. (2023) is GD1, a factor for differentiation of female gametocytes. Parasites lacking GD1 show a sex ratio shift towards males, which were infertile. Interaction partners of GD1, as identified by co-immunoprecipitation assays, included CCR4-NOT complex members, e.g., a NOT1-G paralog, as well as CITH, PABP1 and PUF1, hence similar interactors as identified by us for *P. falciparum* MD3 (Russell et al., 2023). Interestingly, the authors claimed *P. berghei* GD1 as an ortholog of *P. falciparum* ZNF4 (see below). Furthermore, the MD3 interactors FD1 and FD2 were reported to be important for *P. berghei* female differentiation and parasites deficient of these proteins produce infertile female gametocytes lacking transcripts for core female markers (Russell et al., 2023). In addition, *P. berghei* mutants deficient of MD1 and MD2 are not capable to form male gametocytes, while the females are fertile with transcriptomes comparable to WT parasites (Russell et al., 2023). MD1 has been recently characterized in *P. falciparum* and was shown to be present in cytoplasmic granules, where it interacts with mRNP complexes (Gomes et al., 2022). The N- and C-termini of the protein define the function of MD1, as the N-terminus can solely specify a male fate, while the C-terminus comprises an OST/HTH/LOTUS domain essential for the development of male gametocytes. Disruption of the *md1* gene results in impaired exflagellation and aberrant morphology of the gametocytes. Strikingly, MD1 shares interaction partners with MD3 like translational repressors and components of CCR4-NOT complex (Gomes et al., 2022). Noteworthy in this context, the MD4 ortholog in *P. falciparum*, termed, ARID, was shown to be a nuclear protein with a crucial role in male gametocyte exflagellation and macrogamete fertility (Kumar, Baranwal, Haile, et al., 2022).

Finally, we confirmed the interaction of MD3 with two epigenetically regulated ZFPs, i.e., RNF1, a RING-finger domain ZFP with putative E3 ubiquitin ligase activity, and the C3H1-ZFP ZNF4. Both ZFPs were originally identified by us in a comparative transcriptomics analysis of TSA-treated immature gametocytes, hence in the same study which enabled us to identify MD3 (Ngwa et al., 2017). ZNF4, which was assigned homologies to GD1 (see above), has important roles in male gametocyte exflagellation by regulating male-enriched genes like ones related to microtubule/cilium morphogenesis (Hanhsen et al., 2022).

Noteworthy, other recent studies have also reported on RNA-binding proteins with roles in male gametogenesis. The RNA-binding protein UIS12 of *P. berghei* is involved in gametocytogenesis with particular impact on exflagellation and hence malaria transmission (Muller et al., 2021). Lack of UIS12 leads to transcriptional downregulation of various known markers of gametocytes and gametes like MiGS, P48745, P28, or PPLP2 as well as various LCCL domain proteins (reviewed in Bennink et al., 2016; Bennink & Pradel, 2021). In addition, the transcript encoding a protein of the gametocyte inner membrane complex (IMC), IMC1j, was affected (Muller et al., 2021). In relevance, the serine/arginine-rich protein kinase SRPK1, which was previously implicated in pre-mRNA splicing, was also recently assigned to male gametogenesis (Kern et al., 2014; Kumar, Baranwal, Leeb, et al., 2022). Parasites lacking SRPK1 were deregulated in genes coding, e.g., for microtubule/cilium morphogenesis-related proteins, including IMC components.

These recent data on regulators of male gametogenesis highlight a link between RNA-binding proteins and proteins involved in IMC morphogenesis. Strikingly, the here identified MD3 interactome of immature gametocytes includes the PIP (Photosensitized 5-iodonaphthalene-1-azide Labeled protein-1 Interacting Proteins) members PIP1 to PIP3, all of which are assigned to the gametocyte IMC. The IMC is a flattened cisterna-like membrane compartment underneath the plasma membrane that is accompanied by

microtubes and important for the falciform shape of *P. falciparum* gametocytes (Dearnley et al., 2012; Kono et al., 2012; Simon et al., 2013; Parkyn Schneider et al., 2017). During gametogenesis, the IMC is disassembled and contributes to plasma membrane restructuring of the newly formed gametes as well as to the formation of nanotubes, tubular cell-to-cell connections of gametes (Rupp et al., 2011; Simon et al., 2013; Sologub et al., 2011). While PIP2 and PIP3 are found in all malaria species, PIP1 is limited to human malaria parasites (Kono et al., 2012). With high expression of PIP1 in early gametocytes, its downregulation results in failure of *P. falciparum* gametocyte maturation as a result of impaired elongation (Parkyn Schneider et al., 2017).

Considering the current state of data, we deduce that while epigenetic mechanisms play a role in the sex determination of *P. falciparum* gametocytes during sexual commitment, the subsequent sexual development necessitates additional regulation of transcripts by RNA-binding proteins. A closely knit network of ZFPs, PUF proteins and translational regulators is involved in both activation and repression of translation, thereby influencing the destiny of the transcript and, consequently, sexual development. Further research is required to ascertain the extent of interaction between these regulators and other protein complexes, such as the IMC proteins mentioned in this context, which also contribute to the maturity and fertility of gametocytes.

4 | MATERIALS AND METHODS

4.1 | Gene identifiers

The following PlasmoDB gene identifiers (gene IDs) are assigned to the genes and proteins investigated in this study: aldolase (PF3D7_1444800); CITH (PF3D7_1474900); falcilysin (PF3D7_1360800); histone H3 (PF3D7_0610400); MD3 (PF3D7_0315600); P25 (PF3D7_1031000); P92 (PF3D7_1364100); P230 (PF3D7_0209000); PABP1 (PF3D7_1224300); Pf39 (PF3D7_1108600); *Pf*AMA1 (PF3D7_1133400); PfFNPA (PF3D7_1451600); PUF1 (PF3D7_0518700); RNF1 (PF3D7_0314700); ZNF4 (PF3D7_1134600).

4.2 | Antibodies

In this study, the following antibodies were used: rabbit polyclonal antisera against HA (Sigma-Aldrich), P230 (Biogenes), P25 (ATCC, Manassas, USA), P92 (Musabyimana et al., 2022), Pf39 (Davids Biotechnology, Regensburg, DE), *P. yoelii* PABP1 (Minns et al., 2018) and *Py*CITH (Bennink et al., 2018); mouse polyclonal antisera against P230 region C (Williamson et al., 1995) and falcilysin (Weißbach et al., 2017); rabbit anti-H3K4me3 antibody (abcam, Cambridge, UK), monoclonal rat anti-HA antibody (Roche, Basel, CH) and mouse anti-GFP antibody (Roche). Mouse antisera against MD3 and RNF1 were generated as described below. The following dilutions were used for IFAs: rabbit anti-P230 (1:200), rabbit anti-P92 (1:200), mouse anti-MD3 (1:20), rabbit anti-P25 (1:200), rabbit anti-Pf39 (1:200) mouse anti-GFP (1:200) and rat anti -HA (1:50). For WB analysis, the following dilutions were used: rat anti-HA (1:500), rabbit anti-HA (1:1000), rabbit anti-Pf39 (1:10,000), mouse anti-GFP (1:1,000), mouse anti-MD3 (1:300), mouse anti-RNF1 (1:1,000), rabbit anti-CITH (1:1,000) and rabbit anti-PABP1 (1:1,000).

4.3 | Bioinformatics

The 3D structure of MD3 was predicted using the Alphafold program (https://alphafold.ebi.ac.uk/; Jumper et al., 2021; Varadi et al., 2022). Single-cell transcriptome data was retrieved from the Malaria Cell Atlas (MCA; https://www.malariacellatlas.org; Howick et al., 2019). Predictions of gene expression and protein properties and function were made using the database PlasmoDB (http://plasmoDB.org; Aurrecoechea et al., 2009); the peak transcript expression of candidate genes was analyzed using table "Transcriptomes of 7 sexual and asexual life stages" (López-Barragán et al., 2011), and sex specificity was predicted using table "Gametocyte Transcriptomes" (Lasonder et al., 2016) of the PlasmoDB database. The gene ontology enrichment (GO) analysis was performed using the ShinyGO 0.77 program (http://bioinformatics.sdstate.edu/go; Ge et al., 2020) with a p-value cut-off of 0.05. A network analysis was conducted using the STRING database (version 11.0; https://string-db.org; Szklarczyk et al., 2019), using default settings, including text mining options and a confidence of 0.4.

4.4 | Parasite culture

The WT NF54 and all generated mutant parasite lines were cultivated in vitro in human blood group A+ erythrocytes as previously described (Ifediba & Vanderberg, 1981). Asexual blood stages and gametocytes were maintained in RPMI 1640/HEPES medium (Gibco; Thermo Fisher Scientific; Waltham, US) supplemented with 10% (v/v) heat inactivated human A+ serum, 50 µg/mL hypoxanthine (Sigma-Aldrich; Taufkirchen, DE) and 10 µg/mL gentamicin (Gibco; Thermo Fisher Scientific). For cultivation of the mutant parasite lines, the selection drug WR99210 (Jacobus Pharmaceutical Company; Princeton, US) was added at a final concentration of 4.0 nM. All cultures were kept at 37°C in an atmosphere of 5% O_2 and 5% CO_2 in N_2. Synchronization of cultures was carried out by repeated 5% sorbitol treatment as described (Lambros & Vanderberg, 1979). For the generation of gametocytes, the cultures with mainly ring stages at high parasitemia were induced by the addition of lysed RBCs for 24 h (Ngwa et al., 2017; Schneweis et al., 1991). Following removal of the lysed RBCs, the culture medium was supplemented with 50 mM N-acetyl glucosamine (GlcNac; Carl Roth, Karlsruhe, DE) for ~5 days to kill the

asexual blood stages (Fivelman et al., 2007). Gametocytes were enriched via Percoll (Cytiva; Washington DC, US) gradient centrifugation as described (Kariuki et al., 1998). Immature gametocytes of stages II–IV were harvested on days 5–10 post-induction, while mature stage V gametocytes were harvested at approximately day 13 post-induction, and the presence of the respective stages was confirmed by Giemsa staining following the manufacturer's protocol (Carl Roth). Gametogenesis was induced by adding xanthurenic acid (XA) in a final concentration of 100 µM dissolved in 1% (v/v) 0.5 M NH_4OH/ddH_2O and incubation for 30 min at room temperature (RT). For transcript knockdown, MD3-HA-*glmS* cultures were kept in a complete medium supplemented with 5 mM GlcN (D-(+)-glucosamine hydrochloride; Sigma-Aldrich). When gametocyte production was induced during transcript knockdown, heparin sulfate (Sigma-Aldrich) with a final concentration of 20 U/mL was used instead of GlcNac to kill the asexual blood stages as described (Miao, Wang, et al., 2013). Reduced protein levels following transcript knockdown were evaluated on a routine basis via WB as described below. For studies on epigenetic regulation, Percoll-enriched immature gametocytes were incubated with 0.26 µM TSA (Cell Signaling Technology, Danvers, US) in 0.5% (v/v) ethanol for 24 h at 37°C. Erythrocyte concentrate and serum from humans were procured from the Department of Transfusion Medicine (University Hospital Aachen, DE). All work with human blood was approved by the University Hospital Aachen Ethics Commission; the donors remained anonymous and serum samples were pooled.

4.5 | Generation of mouse antisera directed against MD3 and RNF1

Recombinant peptides corresponding to portions of MD3 (aa 31–359; Figure 1a) and RNF1 (aa 294–548) were expressed in the *Escherichia coli* system, fused to a maltose-binding tag using the pMAL™c5X-vector (New England Biolabs, Ipswich, US). Briefly, the coding sequences were amplified using gene-specific primers (for primer sequences, see Table S5) and the recombinant proteins were expressed in *E. coli* BL21 (DE3) RIL cells following the manufacturer's protocol (Invitrogen, Karlsruhe, DE). Each protein was then isolated and affinity-purified using an amylose resin according to the manufacturer's protocol (New England Biolabs, Ipswich, US) and the concentration was determined using the Bradford technique. Six weeks old female NMRI mice (Charles River Laboratories, Wilmington, US) were subcutaneously injected with 100 µg of the pure recombinant protein emulsified in Freund's incomplete adjuvant (Sigma-Aldrich) followed by a boost after 4 weeks. At day 10 after the boost, immune sera were collected via heart puncture after anesthetizing the mice by intraperitoneal injection of a mixture of ketamine and xylazine according to the manufacturer's protocol (Sigma-Aldrich). The immune sera of three immunized mice were pooled; sera of three non-immunized mice were used as the negative control. Experiments in mice were approved by the animal welfare committee of the District Council of Cologne, Germany (ref. no. 84–02.05.30.12.097 TVA).

4.6 | Generation of the MD3-HA-*glmS* and PUF1-HA-*glmS* parasite lines

The MD3-HA-*glmS* and PUF1-HA-*glmS* transgenic parasite lines were generated via single-crossover homologous recombination, using vector pSLI-HA-*glmS* (Figure S3a; Birnbaum et al., 2017; Musabyimana et al., 2022; Prommana et al., 2013), which contained a homology block from the 3′ end of the respective genes without the stop codon (for primer sequence, see Table S5). Ligation of the insert and vector backbone was mediated by NotI and XmaI restriction sites. A WT NF54 culture with mainly ring stages was transfected with 100 µg plasmid DNA in transfection buffer via electroporation (310 V, 950 µF, 12 ms; Bio-Rad gene-pulser Xcell). A mock control lacking plasmid DNA was electroporated using transfection buffer and was cultured in medium with and without WR99210. After 6 h of transfection, the integrated parasites were selected using WR99210 at a final concentration of 4 nM. WR99210-resistant parasites appeared at ~21 days post-transfection and the parasites were treated with medium supplemented with 550 µg/mL neomycin (G418 disulfate salt; Sigma-Aldrich) for 2 weeks to remove WT NF54 parasites from the culture. The gDNA was isolated from the transgenic parasite lines using the NucleoSpin Blood Kit (Macherey-Nagel; Dueren, DE) following the manufacturer's protocol and used as template to verify the successful vector integration by diagnostic PCR (for primer sequence, see Table S5).

4.7 | Generation of the MD3-GFP-BirA parasite lines

The MD3-GFP-BirA parasite lines were generated, using vectors pARL-*pfama1* and *pffnpa*-GFP-BirA (Figure S9a; Musabyimana et al., 2022). The restriction enzymes KpnI and AvrII were used to ligate the insert coding for the full-length *md3* sequence and the vector backbone. The constructed plasmids were then used to transfect WT NF54 parasites as described above. For selection of parasites episomally expressing the MD3-GFP-BirA, WR99210 was added to the cultures in a final concentration of 4 nM and successful uptake of the vector was confirmed by diagnostic PCR (for primer sequences, see Table S5).

4.8 | Indirect immunofluorescence assay

Parasite cultures containing mixed asexual blood stages and gametocytes of WT NF54 as well as lines MD3-HA-*glmS*, MD3-*pfama1*-GFP-BirA and MD3-*pffnpa*-GFP-BirA were coated on glass slides as cell monolayers and then air-dried. After fixation in methanol at −80°C for 10 min, the cells were serially incubated in 0.01% (w/v)

saponin/0.5% (w/v) BSA/PBS and 1% (v/v) neutral goat serum (Sigma-Aldrich)/PBS for 30 min at RT to facilitate membrane permeabilization and blocking of non-specific binding. The cells were incubated with the primary antibodies diluted in 3% (w/v) BSA/PBS for 2 h at 37°C, washed 3× with PBS and incubated with the secondary antibody for 1 h at 37°C. Following 2× washing with PBS, incubation with the second primary antibody and the corresponding visualization with the second secondary antibody were carried out as described above. The nuclei were stained with Hoechst 33342 staining solution for 2 min at RT (1:5000 in 1× PBS; Sigma-Aldrich). The cells were mounted with anti-fading solution (Citifluor Limited; London, UK), covered with a coverslip and sealed airtight with nail polish. The parasites were visualized by conventional fluorescence microscopy using a Leica DM5500 B (Leica; Wetzlar, DE) microscope. The following secondary antibodies were used: anti-mouse Alexa Fluor 488, anti-rabbit Alexa Fluor 488, anti-rat Alexa Fluor 488, anti-mouse Alexa Fluor 594, anti-rabbit Alexa Fluor 594, (1:1000; Invitrogen Molecular Probes; Eugene, US, or Sigma-Aldrich); further Alexa Fluor 594 streptavidin (1:500; Invitrogen) was used. Alternatively, the asexual blood stages were stained with 0.01% (w/v) Evans Blue (Sigma-Aldrich)/PBS for 3 min at RT followed by 5 min washing with PBS. Images were processed using the Adobe Photoshop CS software.

4.9 | Subcellular fractionation

Percoll-purified immature gametocytes of WT NF54 and the MD3-HA-*glmS* line were lysed using lysis buffer (20 mM HEPES (pH 7.8), 10 mM KCl, 1 mM EDTA, 1 mM dithiothreitol (DTT), 1 mM PMSF, 1% (v/v) Triton X-100), with addition of protease inhibitor cocktail (complete EDTA-free; Roche) and incubated for 10 min on ice. The lysates were carefully centrifuged at 2500×*g* for 5 min at 4°C, the cytosolic proteins were harvested with the supernatant and stored at −80°C. Following washing of the remaining pellet with the lysis buffer, nuclear proteins were extracted with twice the volume of the extraction buffer (20 mM HEPES (pH 7.8), 800 mM KCl, 1 mM EDTA, 1 mM DTT, and 1 mM PMSF), after addition of the protease inhibitor cocktail. Following incubation for 30 min, while rotating at 4°C, the extract was cleared by centrifugation at 13,000×*g* for 30 min at 4°C. Finally, the supernatants were diluted in a 1:1 ratio with dilution buffer (20 mM HEPES (pH 7.8); 1 mM EDTA; 1 mM DTT; 30% (v/v) glycerol) and stored at −80°C. The individual fractions were subjected to WB as described below.

4.10 | Co-immunoprecipitation assay

Percoll-purified immature gametocytes of WT NF54 and the transgenic lines MD3-HA-*glmS*, ZNF4-HA-*glmS* (Hanhsen et al., 2022) and PUF1-HA-*glmS* were lysed with RIPA buffer (150 mM NaCl, 1% (v/v) Triton X-100, 0.5% (w/v) sodium deoxycholate, 0.1% (w/v) SDS, 50 mM Tris buffer). Following incubation on ice for 15 min, three sessions of sonication were applied to each sample (30 s/50% and 0.5 cycles). After centrifugation at 16,000×*g* for 10 min at 4°C, the supernatant was incubated with 5% (v/v) pre-immune rabbit or rat sera for 30 min, followed by incubation with 20 µL of protein G-beads (Roche) for 1 h on a rotator at 4°C. Following centrifugation at 3500×*g* for 5 min at 4°C, the supernatant was incubated for 1 h at 4°C with 5% (v/v) monoclonal rat or polyclonal rabbit anti-HA antisera. Afterward, a volume of 30 µL protein G-beads was added and kept on rotation overnight at 4°C. The beads were centrifuged at 3500×*g* for 5 min at 4°C and sequentially washed with ice cold RIPA buffer and PBS for five times. The beads were resuspended in an equal volume of loading buffer and the samples were subjected to WB analysis as described below.

4.11 | Western blotting

Asexual blood stage parasites of WT NF54 and lines MD3-HA-*glmS*, MD3-*pfama1*-GFP-BirA and PUF1-HA-*glmS* were harvested from mixed or synchronized cultures, while gametocytes of WT NF54, or lines MD3-HA-*glmS*, MD3-*pffnpa*-GFP-BirA and PUF1-HA-*glmS* were enriched by Percoll purification. The infected RBCs (iRBCs) were lysed with 0.05% (w/v) saponin/PBS for 10 min at 4°C to release the parasites, then washed with PBS, and resuspended in lysis buffer (0.5% (v/v) Triton X-100, 4% (w/v) SDS in PBS) supplemented with protease inhibitor cocktail. After adding 5× SDS-PAGE loading buffer containing 25 mM DTT, the lysates were heat-denatured for 10 min at 95°C. Lysates were separated via SDS-PAGE and transferred to Hybond ECL nitrocellulose membranes (Amersham Biosciences, Buckinhamshire, UK) following the manufacturer's protocol. Non-specific binding sites were blocked by incubation with 5% (w/v) skim milk and 1% (w/v) BSA in Tris buffer (pH 7.5) for 1 h at 4°C. For immunodetection, membranes were incubated overnight at 4°C with the primary antibody in 3% (w/v) skim milk/TBS. The membranes were washed 3× each with 3% (w/v) skim milk/TBS and 3% (w/v) skim milk/0.1% (v/v) Tween/TBS and then incubated for 1 h at RT with goat anti-mouse, anti-rabbit or anti-rat alkaline phosphatase-conjugated secondary antibodies (dilution 1:10,000, Sigma-Aldrich) in 3% (w/v) skim milk/TBS. The membranes were developed in an NBT/BCIP solution (nitroblue tetrazolium chloride/5-bromo-4-chloro-3-indoxyl phosphate; Roche) for up to 20 min at RT. For the detection of biotinylated proteins, the blocking step was performed overnight at 4°C in 5% (w/v) skim milk/TBS and the membrane was washed 5× with 1× TBS before incubation with streptavidin-conjugated alkaline phosphatase (dilution 1:1000; Sigma-Aldrich) in 5% (w/v) BSA/TBS for 1 h at RT. Blots were scanned and processed using the Adobe Photoshop CS software. Band intensities were measured using the ImageJ program version 1.51f (https://imagej.net).

4.12 | Asexual blood stage replication assay

Asexual blood stage cultures of line MD3-HA-*glmS* or WT NF54 were tightly synchronized and set to an initial parasitemia of 0.25% ring stages. The cultures were then continuously treated with 5 mM

GlcN for transcript knockdown. Untreated cultures were used for control. Giemsa-stained thin blood smears were prepared at 0, 24, 48, 72 and 96 h post-seeding. At each time point, the parasitemia was determined microscopically at 1000-fold magnification by counting the percentage of parasites in 1000 RBCs. Blood stages (ring, trophozoites, schizonts) present in the cultures were identified at each time point by counting 50 iRBCs per setting. For each assay, three experiments were performed, each in triplicate. Data analysis was performed using MS Excel 2016 and GraphPad Prism 5.

4.13 | Gametocyte development assay

Tightly synchronized ring stage parasite cultures of line MD3-HA-*glmS* and WT NF54 at a parasitemia of 7.5% were induced with lysed RBCs for 24 h. The cultures were subsequently maintained in cell culture medium supplemented with 20 U/mL heparin sulfate to kill the asexual blood stages for 4 days. The cultures were then treated with 5 mM GlcN for transcript knockdown until day 13. Untreated cultures were used as control. Giemsa-stained thin blood smears were prepared at days 3, 5, 7, 9, 11 and 13 post-induction. Gametocytemia was determined per 1000 RBCs and the numbers of gametocyte stages II to V were quantified microscopically for 50 iRBCs per setting. For each assay, three experiments were performed, each in triplicate. Data analysis was performed using MS Excel 2016 and GraphPad Prism 5.

4.14 | Exflagellation assay

Tightly synchronized ring stage parasite cultures of line MD3-HA-*glmS* and WT NF54 at a parasitemia of 7.5% were induced by addition of lysed RBCs for 24 h. Subsequently, the asexual blood stages were killed by 50 mM GlcNac for 2 days followed by 20 U/mL heparin sulfate for the next 2 days. On day 7 post-induction, 5 mM GlcN was added for 4 days for transcript knockdown. Untreated cultures were used for control. The cultures were allowed to recover for a period of 2 days prior to the exflagellation assays. On days 13 and 15 post-induction, exflagellation of male gametocytes was investigated, using light microscopy. For this, the gametocyte cultures of the four setups were adjusted to total RBC numbers and the numbers of mature gametocytes were determined for each culture by Giemsa staining. For gametocyte activation, 100 µL of each gametocyte culture was activated by addition of 100 µM XA for 15 min at RT. The number of exflagellation centers was counted at 400-fold magnification in 30 optical fields in triplicate, and the results were adjusted to the numbers of mature gametocytes as evaluated prior to activation. Data analysis was done using GraphPad Prism 5.

4.15 | Sex shift assay

The sex shift assay was carried out using tightly synchronized schizont stages at a parasitemia of 0.5%. Parasites were treated with 5 mM GlcN for 72 h before gametocyte induction and the treatment was continued until day 9 post-induction. Following induction with lysed RBCs for 24 h, the culture was treated with 20 U/mL heparin sulfate for 4 days to kill the asexual blood stages. Untreated MD3-HA-*glmS* and GlcN-treated and untreated WT NF54 were used as negative controls. On day 9 post-induction, the parasites were immunolabeled with antisera directed against P25 (to mark female gametocytes) and P230 (to mark gametocytes of both sexes) as described above. A total of 50 P230-positive gametocytes was counted in quadruplicate for each culture and the percentage of P25-positive gametocytes was calculated. Data analysis was done using MS Excel 2016.

4.16 | Preparation of samples for BioID analysis

Highly synchronized ring stage parasite cultures of line MD3-*pfama1*-GFP-BirA and Percoll-purified immature gametocyte cultures of line MD3-*pffnpa*-GFP-BirA as well as WT NF54 as control were treated with biotin (Sigma-Aldrich), at a final concentration of 50 µM for 24 h. The RBCs were then lysed with 0.05% (w/v) saponin and the parasites were resuspended in 100 µL binding buffer (Tris buffer containing 1% (v/v) Triton X-100 and protease inhibitor). The samples were sonicated on ice (2 × 60 pulses at 30% duty cycle) and another 100 µL of ice-cold binding buffer was added. After a second session of sonification, cell debris was pelleted by centrifugation (5 min, 16,000×*g*, 4°C). The supernatant was mixed with pre-equilibrated streptavidin sepharose magnetic beads (Cytiva) in a low-binding reaction tube. Incubation was performed with slow end-over-end mixing overnight at 4°C. The beads were washed 6× with 500 µL washing buffer (3×: RIPA buffer containing 0.03% (w/v) SDS, followed by 3× 25 mM Tris buffer (pH 7.5)) and were resuspended in 45 µL elution buffer (1% (w/v) SDS/5 mM biotin in Tris buffer (pH 7.5)), followed by an incubation for 5 min at 95°C. The supernatant was transferred to a new reaction tube and stored at −20°C. Three independent samples were collected from each of the two lines and mass spectrometric analysis was performed on streptavidin-purified protein samples. Pull-down samples from WT NF54 lysates were used as a negative control.

4.17 | Proteolytic digestion

Samples were processed by single-spot solid-phase-enhanced sample preparation (SP3) as described before (Hughes et al., 2014; Sielaff et al., 2017). In brief, proteins bound to the streptavidin beads were released by incubating the samples for 5 min at 95°C in an SDS-containing buffer (1% (w/v) SDS, 5 mM biotin in water/Tris buffer, pH 8.0). After elution, proteins were reduced and alkylated, using DTT and iodoacetamide (IAA), respectively. Afterward, 2 µL of carboxylate-modified paramagnetic beads (Sera-Mag Speed Beads, GE Healthcare; Chicago, US; 0.5 µg solids/µL in water; Hughes et al., 2014) were added to the samples. After adding acetonitrile to a final concentration of 70% (v/v), samples were allowed to settle

at RT for 20 min. Subsequently, beads were washed twice with 70% (v/v) ethanol in water and once with acetonitrile. The beads were resuspended in 50 mM NH_4HCO_3 supplemented with trypsin (Mass Spectrometry Grade, Promega; Madison, US) at an enzyme-to-protein ratio of 1:25 (w/w) and incubated overnight at 37°C. After overnight digestion, acetonitrile was added to the samples to reach a final concentration of 95% (v/v) followed by incubation at RT for 20 min. To increase the yield, supernatants derived from this initial peptide-binding step were additionally subjected to the SP3 peptide purification procedure (Sielaff et al., 2017). Each sample was washed with acetonitrile. To recover bound peptides, paramagnetic beads from the original sample and corresponding supernatants were pooled in 2% (v/v) dimethyl sulfoxide (DMSO) in water and sonicated for 1 min. After 2 min of centrifugation at 14,000×*g* and 4°C, supernatants containing tryptic peptides were transferred into a glass vial and acidified with 0.1% (v/v) formic acid.

4.18 | Liquid chromatography-mass spectrometry (LC-MS) analysis

Tryptic peptides were separated using an Ultimate 3000 RSLCnano LC system (Thermo Fisher Scientific) equipped with a PEPMAP100 C18 5 µm 0.3×5 mm trap (Thermo Fisher Scientific) and an HSS-T3 C18 1.8 µm, 75 µm×250 mm analytical reversed-phase column (Waters Corporation; Milford, US). Mobile phase A was water containing 0.1% (v/v) formic acid and 3% (v/v) DMSO. Peptides were separated by running a gradient of 2%–35% mobile phase B (0.1% (v/v) formic acid, 3% (v/v) DMSO in ACN) over 40 min at a flow rate of 300 nL/min. Total analysis time was 60 min including wash and column re-equilibration steps. Column temperature was set to 55°C. Mass spectrometric analysis of eluting peptides was conducted on an Orbitrap Exploris 480 (Thermo Fisher Scientific) instrument platform. Spray voltage was set to 1.8 kV, the funnel RF level to 40, and heated capillary temperature was at 275°C. Data were acquired in data-dependent acquisition (DDA) mode targeting the 10 most abundant peptides for fragmentation (Top10). Full MS resolution was set to 120,000 at m/z 200 and full MS automated gain control (AGC) target to 300% with a maximum injection time of 50 ms. Mass range was set to m/z 350–1500. For MS2 scans, the collection of isolated peptide precursors was limited by an ion target of 1×10^5 (AGC target value of 100%) and maximum injection times of 25 ms. Fragment ion spectra were acquired at a resolution of 15,000 at m/z 200. Intensity threshold was kept at 1E4. Isolation window width of the quadrupole was set to 1.6 m/z and normalized collision energy was fixed at 30%. All data were acquired in profile mode using positive polarity. Each sample was analyzed in three technical replicates.

4.19 | Data analysis and label-free quantification

DDA raw data acquired with the Exploris 480 were processed with MaxQuant (version 2.0.1; Cox & Mann, 2008; Cox et al., 2014), using the standard settings and label-free quantification (LFQ) enabled for each parameter group, i.e., control and affinity-purified samples (LFQ min ratio count 2, stabilize large LFQ ratios disabled, match-between-runs). Data were searched against the forward and reverse sequences of the *P. falciparum* proteome (UniProtKB/TrEMBL, 5445 entries, UP000001450, released April 2020) and a list of common contaminants. For peptide identification, trypsin was set as protease allowing two missed cleavages. Carbamidomethylation was set as fixed and oxidation of methionine as well as acetylation of protein N-termini as variable modifications. Only peptides with a minimum length of 7 amino acids were considered. Peptide and protein false discovery rates (FDR) were set to 1%. In addition, proteins had to be identified by at least two peptides. Statistical analysis of the data was conducted using Student's *t*-test, which was corrected by the Benjamini-Hochberg (BH) method for multiple hypothesis testing (FDR of 0.01). In addition, proteins in the affinity-enriched samples had to be identified in all three biological replicates and show at least a two-fold enrichment compared to the controls. The datasets of protein hits were further edited by verification of the gene IDs and gene names via the PlasmoDB database (www.plasmodb.org; Aurrecoechea et al., 2009). PlasmoDB gene IDs were extracted from the fasta headers provided by mass spectrometry and verified manually. Once an initial list of significantly enriched proteins had been established, proteins with a putative signal peptide were excluded.

4.20 | Statistical analysis

Data are presented as mean ± SD. Statistical differences were determined using one-way ANOVA with post hoc Bonferroni multiple comparison test or unpaired two-tailed Student's *t*-test, as indicated. The *p*-values < 0.05 were considered statistically significant. Significances were calculated using GraphPad Prism 5 and are represented in the figures as follows: $^*p<0.05$; $^{**}p<0.01$; $^{***}p<0.001$.

AUTHOR CONTRIBUTIONS

Afia Farrukh: Investigation; formal analysis; conceptualization; methodology; visualization; writing – original draft. **Jean Pierre Musabyimana:** Investigation; formal analysis; methodology; software; visualization; data curation. **Ute Distler:** Data curation; resources; software; formal analysis; validation; methodology. **Vanessa Jil Mahlich:** Formal analysis; methodology. **Julius Mueller:** Formal analysis; data curation. **Fabian Bick:** Methodology; formal analysis. **Stefan Tenzer:** Investigation; funding acquisition; methodology; project administration; supervision; software; resources. **Gabriele Pradel:** Conceptualization; investigation; funding acquisition; writing – review and editing; validation; project administration; data curation; supervision; resources; visualization. **Che Julius Ngwa:** Conceptualization; investigation; funding acquisition; writing – original draft; methodology; formal analysis; project administration; supervision; data curation.

ACKNOWLEDGMENTS

The authors acknowledge funding by the Deutsche Forschungsgemeinschaft (DFG; project grants PR905/15-1 and PR905/20-1 to GP and NG170/1-1 to CJN; DFG priority program SPP 2225 grants PR905/19-1 to GP, and TE599/9-1 to ST). AF and JPM were supported by stipends from the Deutscher Akademischer Austauschdienst (DAAD). Open Access funding enabled and organized by Projekt DEAL.

DATA AVAILABILITY STATEMENT

The mass spectrometry proteomics data have been deposited to the ProteomeXchange Consortium (http://proteomecentral.proteomexchange.org) via the jPOST partner repository (Vizcaino et al., 2013) with the dataset identifiers PXD042976 (ProteomeXchange) and JPST002199 (jPOST).

ETHICS STATEMENT

This study used erythrocytes and serum from humans, which were procured from the Department of Transfusion Medicine (University Hospital Aachen, DE). All work with human blood was approved by the University Hospital Aachen Ethics commission; the donors remained anonymous and serum samples were pooled.

ORCID

Gabriele Pradel https://orcid.org/0000-0003-2264-5558

REFERENCES

Aurrecoechea, C., Brestelli, J., Brunk, B.P., Dommer, J., Fischer, S., Gajria, B. et al. (2009) PlasmoDB: a functional genomic database for malaria parasites. *Nucleic Acids Research*, 37, D539–D543. Available from: https://doi.org/10.1093/nar/gkn814

Balbin, J.M., Heinemann, G.K., Yeoh, L.M., Gilberger, T.W., Armstrong, M., Duffy, M.F. et al. (2023) Characterisation of PfCZIF1 and PfCZIF2 in *Plasmodium falciparum* asexual stages. *International Journal for Parasitology*, 53, 27–41. Available from: https://doi.org/10.1016/j.ijpara.2022.09.008

Bancells, C., Llora-Batlle, O., Poran, A., Notzel, C., Rovira-Graells, N., Elemento, O. et al. (2019) Revisiting the initial steps of sexual development in the malaria parasite *Plasmodium falciparum*. *Nature Microbiolology*, 4, 144–154. Available from: https://doi.org/10.1038/s41564-018-0291-7

Banerjee, C., Nag, S., Goyal, M., Saha, D., Siddiqui, A.A., Mazumder, S. et al. (2023) Nuclease activity of *Plasmodium falciparum* Alba family protein PfAlba3. *Cell Reports*, 42, 112292. Available from: https://doi.org/10.1016/j.celrep.2023.112292

Baumgarten, S., Bryant, J.M., Sinha, A., Reyser, T., Preiser, P.R., Dedon, P.C. et al. (2019) Transcriptome-wide dynamics of extensive m(6) A mRNA methylation during *Plasmodium falciparum* blood-stage development. *Nature Microbiology*, 4, 2246–2259. Available from: https://doi.org/10.1038/s41564-019-0521-7

Bennink, S., Kiesow, M.J. & Pradel, G. (2016) The development of malaria parasites in the mosquito midgut. *Cellular Microbiology*, 18, 905–918. Available from: https://doi.org/10.1111/cmi.12604

Bennink, S. & Pradel, G. (2019) The molecular machinery of translational control in malaria parasites. *Molecular Microbiology*, 112, 111372. Available from: https://doi.org/10.1111/mmi.14388

Bennink, S. & Pradel, G. (2021) Vesicle dynamics during the egress of malaria gametocytes from the red blood cell. *Molecular and Biochemical Parasitology*, 234, 1658–1673. Available from: https://doi.org/10.1016/j.molbiopara.2021.111372

Bennink, S., von Bohl, A., Ngwa, C.J., Henschel, L., Kuehn, A., Pilch, N. et al. (2018) A seven-helix protein constitutes stress granules crucial for regulating translation during human-to-mosquito transmission of *Plasmodium falciparum*. *PLoS Pathogens*, 14, e1007249. Available from: https://doi.org/10.1371/journal.ppat.1007249

Birnbaum, J., Flemming, S., Reichard, N., Soares, A.B., Mesen-Ramirez, P., Jonscher, E. et al. (2017) A genetic system to study *Plasmodium falciparum* protein function. *Nature Methods*, 14, 450–456. Available from: https://doi.org/10.1038/nmeth.4223

Brancucci, N.M.B., Bertschi, N.L., Zhu, L., Niederwieser, I., Chin, W.H., Wampfler, R. et al. (2014) Heterochromatin protein 1 secures survival and transmission of malaria parasites. *Cell Host & Microbe*, 16, 165–176. Available from: https://doi.org/10.1016/j.chom.2014.07.004

Bunnik, E.M., Batugedara, G., Saraf, A., Prudhomme, J., Florens, L. & Le Roch, K.G. (2016) The mRNA-bound proteome of the human malaria parasite *Plasmodium falciparum*. *Genome Biology*, 17, 147. Available from: https://doi.org/10.1186/s13059-016-1014-0

Chene, A., Vembar, S.S., Riviere, L., Lopez-Rubio, J.J., Claes, A., Siegel, T.N. et al. (2012) PfAlbas constitute a new eukaryotic DNA/RNA-binding protein family in malaria parasites. *Nucleic Acids Research*, 40, 3066–3077. Available from: https://doi.org/10.1093/nar/gkr1215

Coleman, B.I., Skillman, K.M., Jiang, R.H.Y., Childs, L.M., Altenhofen, L.M., Ganter, M. et al. (2014) A *Plasmodium falciparum* histone deacetylase regulates antigenic variation and gametocyte conversion. *Cell Host & Microbe*, 16, 177–186. Available from: https://doi.org/10.1016/j.chom.2014.06.014

Cox, J., Hein, M.Y., Luber, C.A., Paron, I., Nagaraj, N. & Mann, M. (2014) Accurate proteome-wide label-free quantification by delayed normalization and maximal peptide ratio extraction, termed MaxLFQ. *Molecular & Cellular Proteomics*, 13, 2513–2526. Available from: https://doi.org/10.1074/mcp.M113.031591

Cox, J. & Mann, M. (2008) MaxQuant enables high peptide identification rates, individualized p.p.b.-range mass accuracies and proteome-wide protein quantification. *Nature Biotechnology*, 26, 1367–1372. Available from: https://doi.org/10.1038/nbt.1511

Cui, L., Mharakurwa, S., Ndiaye, D., Rathod, P.K. & Rosenthal, P.J. (2015) Antimalarial drug resistance: literature review and activities and findings of the ICEMR network. *American Journal of Tropical Medicine and Hygiene*, 93, 57–68. Available from: https://doi.org/10.4269/ajtmh.15-0007

Dearnley, M.K., Yeoman, J.A., Hanssen, E., Kenny, S., Turnbull, L., Whitchurch, C.B. et al. (2012) Origin, composition, organization and function of the inner membrane complex of *Plasmodium falciparum* gametocytes. *Journnal of Cell Science*, 125, 2053–2063. Available from: https://doi.org/10.1242/jcs.099002

Filarsky, M., Fraschka, S.A., Niederwieser, I., Brancucci, N.M.B., Carrington, E., Carrio, E. et al. (2018) GDV1 induces sexual commitment of malaria parasites by antagonizing HP1-dependent gene silencing. *Science*, 359, 1259–1263. Available from: https://doi.org/10.1126/science.aan6042

Fivelman, Q.L., McRobert, L., Sharp, S., Taylor, C.J., Saeed, M., Swales, C.A. et al. (2007) Improved synchronous production of *Plasmodium falciparum* gametocytes in vitro. *Molecular and Biochemical Parasitology*, 154, 119–123. Available from: https://doi.org/10.1016/j.molbiopara.2007.04.008

Furuya, T., Mu, J., Hayton, K., Liu, A., Duan, J., Nkrumah, L. et al. (2005) Disruption of a *Plasmodium falciparum* gene linked to male sexual development causes early arrest in gametocytogenesis. *Proceedings of the National Academy of Sciences of the United States of America*, 102, 16813–16818. Available from: https://doi.org/10.1073/pnas.050185810

Ge, S.X., Jung, D. & Yao, R. (2020) ShinyGO: a graphical gene-set enrichment tool for animals and plants. *Bioinformatics*, 36, 2628–2629. Available from: https://doi.org/10.1093/bioinformatics/btz931

Gomes, A.R., Marin-Menendez, A., Adjalley, S.H., Bardy, C., Cassan, C., Lee, M.C.S. et al. (2022) A transcriptional switch controls sex determination in *Plasmodium falciparum*. *Nature*, 612, 528–533. Available from: https://doi.org/10.1038/s41586-022-05509-z

Goyal, M., Simantov, K. & Dzikowski, R. (2022) Beyond splicing: serine-arginine proteins as emerging multifaceted regulators of RNA metabolism in malaria parasites. *Current Opinion in Microbiology*, 70, 102201. Available from: https://doi.org/10.1016/j.mib.2022.102201

Hanhsen, B., Farrukh, A., Pradel, G. & Ngwa, C.J. (2022) The *Plasmodium falciparum* CCCH zinc finger protein ZNF4 plays an important role in gametocyte exflagellation through the regulation of male enriched transcripts. *Cell*, 11, 1666. Available from: https://doi.org/10.3390/cells11101666

Hart, K.J., Oberstaller, J., Walker, M.P., Minns, A.M., Kennedy, M.F., Padykula, I. et al. (2019) Plasmodium male gametocyte development and transmission are critically regulated by the two putative deadenylases of the CAF1/CCR4/NOT complex. *PLoS Pathogens*, 15, e1007164. Available from: https://doi.org/10.1371/journal.ppat.1007164

Hart, K.J., Power, B.J., Rios, K.T., Sebastian, A. & Lindner, S.E. (2021) The Plasmodium NOT1-G paralogue is an essential regulator of sexual stage maturation and parasite transmission. *PLoS Biology*, 19, e3001434. Available from: https://doi.org/10.1371/journal.pbio.3001434

Howick, V.M., Russell, A.J.C., Andrews, T., Heaton, H., Reid, A.J., Natarajan, K. et al. (2019) The malaria cell atlas: single parasite transcriptomes across the complete Plasmodium life cycle. *Science*, 365, eaaw2619. Available from: https://doi.org/10.1126/science.aaw2619

Hughes, C.S., Foehr, S., Garfield, D.A., Furlong, E.E., Steinmetz, L.M. & Krijgsveld, J. (2014) Ultrasensitive proteome analysis using paramagnetic bead technology. *Molecular Systems Biology*, 10, 757. Available from: https://doi.org/10.15252/msb.20145625

Ifediba, T. & Vanderberg, J.P. (1981) Complete in vitro maturation of *Plasmodium falciparum* gametocytes. *Nature*, 294, 364–366. Available from: https://doi.org/10.1038/294364a0

Josling, G.A., Russell, T.J., Venezia, J., Orchard, L., van Biljon, R., Painter, H.J. et al. (2020) Dissecting the role of PfAP2-G in malaria gametocytogenesis. *Nature Communications*, 11, 1503. Available from: https://doi.org/10.1038/s41467-020-15026-0

Jumper, J., Evans, R., Pritzel, A., Green, T., Figurnov, M., Ronneberger, O. et al. (2021) Highly accurate protein structure prediction with AlphaFold. *Nature*, 596, 583–589. Available from: https://doi.org/10.1038/s41586-021-03819-2

Kafsack, B.F., Rovira-Graells, N., Clark, T.G., Bancells, C., Crowley, V.M., Campino, S.G. et al. (2014) A transcriptional switch underlies commitment to sexual development in malaria parasites. *Nature*, 507, 248–252. Available from: https://doi.org/10.1038/nature12920

Kariuki, M.M., Kiaira, J.K., Mulaa, F.K., Mwangi, J.K., Wasunna, M.K. & Martin, S.K. (1998) *Plasmodium falciparum*: purification of the various gametocyte developmental stages from in vitro-cultivated parasites. *The American Journal of Tropical Medicine and Hygiene*, 4, 505–508. Available from: https://doi.org/10.4269/ajtmh.1998.59.505

Kern, S., Agarwal, S., Huber, K., Gehring, A.P., Strodke, B., Wirth, C.C. et al. (2014) Inhibition of the SR protein-phosphorylating CLK kinases of *Plasmodium falciparum* impairs blood stage replication and malaria transmission. *PLoS One*, 9, e105732. Available from: https://doi.org/10.1371/journal.pone.0105732

Kono, M., Herrmann, S., Loughran, N.B., Cabrera, A., Engelberg, K., Lehmann, C. et al. (2012) Evolution and architecture of the inner membrane complex in asexual and sexual stages of the malaria parasite. *Molecular Biology and Evolution*, 29, 2113–2132. Available from: https://doi.org/10.1093/molbev/mss081

Kumar, S., Baranwal, V.K., Haile, M.T., Oualim, K.M.Z., Abatiyow, B.A., Kennedy, S.Y. et al. (2022) *Pf* ARID regulates *P. falciparum* malaria parasite male gametogenesis and female fertility and is critical for parasite transmission to the mosquito vector. *mBio*, 13, e0057822. Available from: https://doi.org/10.1128/mbio.00578-22

Kumar, S., Baranwal, V.K., Leeb, A.S., Haile, M.T., Oualim, K.M.Z., Hertoghs, N. et al. (2022) PfSRPK1 regulates asexual blood stage Schizogony and is essential for male gamete formation. *Microbiology Spectrum*, 10, e0214122. Available from: https://doi.org/10.1128/spectrum.02141-22

Lal, K., Delves, M.J., Bromley, E., Wastling, J.M., Tomley, F.M. & Sinden, R.E. (2009) Plasmodium male development gene-1 (mdv-1) is important for female sexual development and identifies a polarised plasma membrane during zygote development. *International Journal for Parasitology*, 39, 755–761. Available from: https://doi.org/10.1016/j.ijpara.2008.11.008

Lambros, C. & Vanderberg, J.P. (1979) Synchronization of *Plasmodium falciparum* erythrocytic stages in culture. *Journal of Parasitology*, 65, 418–420. Available from: https://doi.org/10.2307/3280287

Lasonder, E., Rijpma, S.R., van Schaijk, B.C., Hoeijmakers, W.A., Kensche, P.R., Gresnigt, M.S. et al. (2016) Integrated transcriptomic and proteomic analyses of *P. falciparum* gametocytes: molecular insight into sex-specific processes and translational repression. *Nucleic Acids Research*, 44, 6087–6101. Available from: https://doi.org/10.1093/nar/gkw536

Li, Z., Cui, H., Guan, J., Liu, C., Yang, Z. & Yuan, J. (2021) Plasmodium transcription repressor AP2-O3 regulates sex-specific identity of gene expression in female gametocytes. *EMBO Reports*, 22, e51660. Available from: https://doi.org/10.15252/embr.202051660

López-Barragán, M.J., Lemieux, J., Quinones, M., Williamson, K.C., Molina-Cruz, A., Cui, K. et al. (2011) Directional gene expression and antisense transcripts in sexual and asexual stages of *Plasmodium falciparum*. *BMC Genomics*, 12, 587. Available from: https://doi.org/10.1186/1471-2164-12-587

Mair, G.R., Braks, J.A., Garver, L.S., Wiegant, J.C., Hall, N., Dirks, R.W. et al. (2006) Regulation of sexual development of Plasmodium by translational repression. *Science*, 313, 667–669. Available from: https://doi.org/10.1126/science.1125129

Mair, G.R., Lasonder, E., Garver, L.S., Franke-Fayard, B.M., Carret, C.K., Wiegant, J.C. et al. (2010) Universal features of post-transcriptional gene regulation are critical for Plasmodium zygote development. *PLoS Pathogens*, 6, e1000767. Available from: https://doi.org/10.1371/journal.ppat.1000767

Miao, J., Fan, Q., Parker, D., Li, X., Li, J. & Cui, L. (2013) Puf mediates translation repression of transmission-blocking vaccine candidates in malaria parasites. *PLoS Pathogens*, 9, e1003268. Available from: https://doi.org/10.1371/journal.ppat.1003268

Miao, J., Li, J., Fan, Q., Li, X., Li, X. & Cui, L. (2010) The Puf-family RNA-binding protein PfPuf2 regulates sexual development and sex differentiation in the malaria parasite *Plasmodium falciparum*. *Journal of Cell Science*, 123, 1039–1049. Available from: https://doi.org/10.1242/jcs.059824

Miao, J., Wang, Z., Liu, M., Parker, D., Li, X., Chen, X. et al. (2013) *Plasmodium falciparum*: generation of pure gametocyte culture by heparin treatment. *Experimental Parasitology*, 135, 541–545. Available from: https://doi.org/10.1016/j.exppara.2013.09.010

Minns, A.M., Hart, K.J., Subramanian, S., Hafenstein, S. & Lindner, S.E. (2018) Nuclear, cytosolic, and surface-localized poly(a)-binding proteins of *Plasmodium yoelii*. *mSphere*, 3, e00435-17. Available from: https://doi.org/10.1128/msphere.00435-17

Modrzynska, K., Pfander, C., Chappell, L., Yu, L., Suarez, C., Dundas, K. et al. (2017) A knockout screen of ApiAP2 genes reveals networks

of interacting transcriptional regulators controlling the Plasmodium life cycle. *Cell Host & Microbe*, 21, 11–22. Available from: https://doi.org/10.1016/j.chom.2016.12.003

Mora, C., McKenzie, T., Gaw, I.M., Dean, J.M., von Hammerstein, H., Knudson, T.A. et al. (2022) Over half of known human pathogenic diseases can be aggravated by climate change. *Nature Climate Change*, 12, 869–875. Available from: https://doi.org/10.1038/s41558-022-01426-1

Muller, K., Silvie, O., Mollenkopf, H.J. & Matuschewski, K. (2021) Pleiotropic roles for the *Plasmodium berghei* RNA binding protein UIS12 in transmission and oocyst maturation. *Frontiers in Cellular and Infection Microbiology*, 11, 624945. Available from: https://doi.org/10.3389/fcimb.2021.624945

Munoz, E.E., Hart, K.J., Walker, M.P., Kennedy, M.F., Shipley, M.M. & Lindner, S.E. (2017) ALBA4 modulates its stage-specific interactions and specific mRNA fates during *Plasmodium yoelii* growth and transmission. *Molecular Microbiology*, 106, 266–284. Available from: https://doi.org/10.1111/mmi.13762

Musabyimana, J.P., Distler, U., Sassmannshausen, J., Berks, C., Manti, J., Bennink, S. et al. (2022) *Plasmodium falciparum* S-Adenosylmethionine synthetase is essential for parasite survival through a complex interaction network with cytoplasmic and nuclear proteins. *Microorganisms*, 10, 1419. Available from: https://doi.org/10.3390/microorganisms10071419

Ngwa, C.J., Farrukh, A. & Pradel, G. (2021) Zinc finger proteins of *Plasmodium falciparum*. *Cellular Microbiology*, 23, e13387. Available from: https://doi.org/10.1111/cmi.13387

Ngwa, C.J., Kiesow, M.J., Papst, O., Orchard, L.M., Filarsky, M., Rosinski, A.N. et al. (2017) Transcriptional profiling defines histone acetylation as a regulator of gene expression during human-to-mosquito transmission of the malaria parasite *Plasmodium falciparum*. *Frontiers in Cellular and Infection Microbiology*, 7, 320. Available from: https://doi.org/10.3389/fcmb.2017.00320

Parkyn Schneider, M., Liu, B., Glock, P., Suttie, A., McHugh, E., Andrew, D. et al. (2017) Disrupting assembly of the inner membrane complex blocks *Plasmodium falciparum* sexual stage development. *PLoS Pathogens*, 13, e1006659. Available from: https://doi.org/10.1371/journal.ppat.1006659

Ponzi, M., Sidén-Kiamos, I., Bertuccini, L., Currà, C., Kroeze, H., Camarda, G. et al. (2009) Egress of *Plasmodium berghei* gametes from their host erythrocyte is mediated by the MDV-1/PEG3 protein. *Cellular Microbiology*, 11, 1272–1288. Available from: https://doi.org/10.1111/j.1462-5822.2009.01331.x

Poran, A., Notzel, C., Aly, O., Mencia-Trinchant, N., Harris, C.T., Guzman, M.L. et al. (2017) Single-cell RNA sequencing reveals a signature of sexual commitment in malaria parasites. *Nature*, 551, 95–99. Available from: https://doi.org/10.1038/nature24280

Prommana, P., Uthaipibull, C., Wongsombat, C., Kamchonwongpaisan, S., Yuthavong, Y., Knuepfer, E. et al. (2013) Inducible knockdown of Plasmodium gene expression using the glmS ribozyme. *PLoS One*, 8, e73783. Available from: https://doi.org/10.1371/journal.pone.0073783

Reddy, B.P., Shrestha, S., Hart, K.J., Liang, X., Kemirembe, K., Cui, L. et al. (2015) A bioinformatic survey of RNA-binding proteins in Plasmodium. *BMC Genomics*, 16, 890. Available from: https://doi.org/10.1186/s12864-015-2092-1

Rupp, I., Sologub, L., Williamson, K.C., Scheuermayer, M., Reininger, L., Doerig, C. et al. (2011) Malaria parasites form filamentous cell-to-cell connections during reproduction in the mosquito midgut. *Cell Research*, 21, 683–696. Available from: https://doi.org/10.1038/cr.2010.176

Russell, A.J.C., Sanderson, T., Bushell, E., Talman, A.M., Anar, B., Girling, G. et al. (2023) Regulators of male and female sexual development are critical for the transmission of a malaria parasite. *Cell Host & Microbe*, 31, 305–319. Available from: https://doi.org/10.1016/j.chom.2022.12.011

Sanders, P.R., Gilson, P.R., Cantin, G.T., Greenbaum, D.C., Nebl, T., Carucci, D.J. et al. (2005) Distinct protein classes including novel merozoite surface antigens in raft-like membranes of *Plasmodium falciparum*. *Journal of Biological Chemistry*, 280, 40169–40176. Available from: https://doi.org/10.1074/jbc.M509631200

Sassmannshausen, J., Bennink, S., Distler, U., Küchenhoff, J., Minns, A.M., Lindner, S.E. et al. (2023) Comparative proteomics of vesicles essential for the egress of *Plasmodium falciparum* gametocytes from red blood cells. *Molecular Microbiology*. Available from: https://doi.org/10.1111/mmi.15125

Schneweis, S., Maier, W.A. & Seitz, H.M. (1991) Haemolysis of infected erythrocytes—a trigger for formation of *Plasmodium falciparum* gametocytes? *Parasitology Research*, 77, 458–460. Available from: https://doi.org/10.1007/BF00931646

Scholz, S.M., Simon, N., Lavazec, C., Dude, M.A., Templeton, T.J. & Pradel, G. (2008) PfCCp proteins of *Plasmodium falciparum*: gametocyte-specific expression and role in complement-mediated inhibition of exflagellation. *International Journal of Parasitology*, 38, 327–340. Available from: https://doi.org/10.1016/j.ijpara.2007.08.009

Shang, X., Shen, S., Tang, J., He, X., Zhao, Y., Wang, C. et al. (2021) A cascade of transcriptional repression determines sexual commitment and development in *Plasmodium falciparum*. *Nucleic Acids Research*, 49, 9264–9279. Available from: https://doi.org/10.1093/nar/gkab683

Shrestha, S., Li, X., Ning, G., Miao, J. & Cui, L. (2016) The RNA-binding protein Puf1 functions in the maintenance of gametocytes in *Plasmodium falciparum*. *Journal of Cell Science*, 129, 3144–3152. Available from: https://doi.org/10.1242/jcs.186908

Sielaff, M., Kuharev, J., Bohn, T., Hahlbrock, J., Bopp, T., Tenzer, S. et al. (2017) Evaluation of FASP, SP3, and iST protocols for proteomic sample preparation in the low microgram range. *Journal of Proteome Research*, 16, 4060–4072. Available from: https://doi.org/10.1021/acs.jproteome.7b00433

Simon, N., Lasonder, E., Scheuermayer, M., Kuehn, A., Tews, S., Fischer, R. et al. (2013) Malaria parasites co-opt human factor H to prevent complement-mediated lysis in the mosquito midgut. *Cell Host & Microbe*, 13, 29–41. Available from: https://doi.org/10.1016/j.chom.2012.11.013

Sinha, A., Baumgarten, S., Distiller, A., McHugh, E., Chen, P., Singh, M. et al. (2021) Functional characterization of the m(6)A-dependent translational modulator PfYTH.2 in the human malaria parasite. *MBio*, 12, e00661-21. Available from: https://doi.org/10.1128/mbio.00661-21

Sinha, A., Hughes, K.R., Modrzynska, K.K., Otto, T.D., Pfander, C., Dickens, N.J. et al. (2014) A cascade of DNA-binding proteins for sexual commitment and development in Plasmodium. *Nature*, 507, 253–257. Available from: https://doi.org/10.1038/nature12970

Smith, T.G., Lourenco, P., Carter, R., Walliker, D. & Ranford-Cartwright, L.C. (2000) Commitment to sexual differentiation in the human malaria parasite, *Plasmodium falciparum*. *Parasitology*, 121, 127–133. Available from: https://doi.org/10.1017/s0031182099006265

Sologub, L., Kuehn, A., Kern, S., Przyborski, J., Schillig, R. & Pradel, G. (2011) Malaria proteases mediate inside-out egress of gametocytes from red blood cells following parasite transmission to the mosquito. *Cellular Microbiology*, 13, 897–912. Available from: https://doi.org/10.1111/j.1462-5822.2011.01588.x

Szklarczyk, D., Gable, A.L., Lyon, D., Junge, A., Wyder, S., Huerta-Cepas, J. et al. (2019) STRING v11: protein-protein association networks with increased coverage, supporting functional discovery in genome-wide experimental datasets. *Nucleic Acids Research*, 47, D607–D613. Available from: https://doi.org/10.1093/nar/gky1131

Tarique, M., Ahmad, M., Ansari, A. & Tuteja, R. (2013) *Plasmodium falciparum* DOZI, an RNA helicase interacts with eIF4E. *Gene*, 522, 46–59. Available from: https://doi.org/10.1016/j.gene.2013.03.063

Usui, M., Prajapati, S.K., Ayanful-Torgby, R., Acquah, F.K., Cudjoe, E., Kakaney, C. et al. (2019) *Plasmodium falciparum* sexual

differentiation in malaria patients is associated with host factors and GDV1-dependent genes. *Nature Communications*, 10, 2140. Available from: https://doi.org/10.1038/s41467-019-10172-6

van Biljon, R., van Wyk, R., Painter, H.J., Orchard, L., Reader, J., Niemand, J. et al. (2019) Hierarchical transcriptional control regulates *Plasmodium falciparum* sexual differentiation. *BMC Genomics*, 20, 920. Available from: https://doi.org/10.1186/s12864-019-6322-9

Varadi, M., Anyango, S., Deshpande, M., Nair, S., Natassia, C., Yordanova, G. et al. (2022) AlphaFold protein structure database: massively expanding the structural coverage of protein-sequence space with high-accuracy models. *Nucleic Acids Research*, 50, D439–D444. Available from: https://doi.org/10.1093/nar/gkab1061

Vembar, S.S., Macpherson, C.R., Sismeiro, O., Coppee, J.Y. & Scherf, A. (2015) The PfAlba1 RNA-binding protein is an important regulator of translational timing in *Plasmodium falciparum* blood stages. *Genome Biology*, 16, 212. Available from: https://doi.org/10.1186/s13059-015-0771-5

Vizcaino, J.A., Cote, R.G., Csordas, A., Dianes, J.A., Fabregat, A., Foster, J.M. et al. (2013) The PRoteomics IDEntifications (PRIDE) database and associated tools: status in 2013. *Nucleic Acids Research*, 41, D1063–D1069. Available from: https://doi.org/10.1093/nar/gks1262

Weißbach, T., Golzmann, A., Bennink, S., Pradel, G. & Ngwa, C.J. (2017) Transcript and protein expression analysis of proteases in the blood stages of *Plasmodium falciparum*. *Experimental Parasitology*, 180, 33–44. Available from: https://doi.org/10.1016/j.exppara.2017.03.006

WHO World Malaria Report. (2023). https://www.who.int/teams/global-malaria-programme/reports/world-malaria-report-2022 (29.06.2023, 17:00).

Williamson, K.C., Criscio, M.D. & Kaslow, D.C. (1993) Cloning and expression of the gene for *Plasmodium falciparum* transmission-blocking target antigen, Pfs230. *Molecular and Biochemical Parasitology*, 58, 355–358. Available from: https://doi.org/10.1016/0166-6851(93)90058-6

Williamson, K.C., Keister, D.B., Muratova, O. & Kaslow, D.C. (1995) Recombinant Pfs230, a *Plasmodium falciparum* gametocyte protein, induces antisera that reduce the infectivity of *Plasmodium falciparum* to mosquitoes. *Molecular and Biochemical Parasitology*, 75, 33–42. Available from: https://doi.org/10.1016/0166-6851(95)02507-3

Xu, Y., Qiao, D., Wen, Y., Bi, Y., Chen, Y., Huang, Z. et al. (2021) PfAP2-G2 is associated to production and maturation of gametocytes in *Plasmodium falciparum* via regulating the expression of PfMDV-1. *Frontiers in Microbiology*, 11, 631444. Available from: https://doi.org/10.3389/fmicb.2020.631444

Yuda, M., Iwanaga, S., Kaneko, I. & Kato, T. (2015) Global transcriptional repression: an initial and essential step for Plasmodium sexual development. *Proceedings of the National Academy of Sciences of the United States of America*, 112, 12824–12829. Available from: https://doi.org/10.1073/pnas.1504389112

Yuda, M., Kaneko, I., Iwanaga, S., Murata, Y. & Kato, T. (2020) Female-specific gene regulation in malaria parasites by an AP2-family transcription factor. *Molecular Microbiology*, 113, 40–51. Available from: https://doi.org/10.1111/mmi.14334

Zhang, C., Li, Z., Cui, H., Jiang, Y., Yang, Z., Wang, X. et al. (2017) Systematic CRISPR-Cas9-mediated modifications of *Plasmodium yoelii* ApiAP2 genes reveal functional insights into parasite development. *MBio*, 8, e01986-17. Available from: https://doi.org/10.1128/mbio.01986-17

SUPPORTING INFORMATION

Additional supporting information can be found online in the Supporting Information section at the end of this article.

How to cite this article: Farrukh, A., Musabyimana, J.P., Distler, U., Mahlich, V.J., Mueller, J., Bick, F. et al. (2023) The *Plasmodium falciparum* CCCH zinc finger protein MD3 regulates male gametocytogenesis through its interaction with RNA-binding proteins. *Molecular Microbiology*, 00, 1–22. Available from: https://doi.org/10.1111/mmi.15215